Title

Consistently dated records from the Greenland GRIP, GISP2 and NGRIP ice cores for the past 104 ka reveal regional millennial-scale δ18O gradients with possible Heinrich event imprint

Authors

Seierstad, Inger K
Abbott, Peter M
Bigler, Matthias
et al.

Publication Date

2014-12-01

DOI

10.1016/j.quascirev.2014.10.032

Peer reviewed

Quaternary Science Reviews 106 (2014) 29–46

Contents lists available at ScienceDirect

Quaternary Science Reviews

journal homepage: www.elsevier.com/locate/quascirev

Consistently dated records from the Greenland GRIP, GISP2 and NGRIP ice cores for the past 104 ka reveal regional millennial-scale $\delta^{18}O$ gradients with possible Heinrich event imprint

Inger K. Seierstad [a, *], Peter M. Abbott [b], Matthias Bigler [c, d], Thomas Blunier [a], Anna J. Bourne [b], Edward Brook [e], Susanne L. Buchardt [a], Christo Buizert [e], Henrik B. Clausen [a, 1], Eliza Cook [b], Dorthe Dahl-Jensen [a], Siwan M. Davies [b], Myriam Guillevic [a, f], Sigfús J. Johnsen [a, 1], Desirée S. Pedersen [a], Trevor J. Popp [a], Sune O. Rasmussen [a], Jeffrey P. Severinghaus [g], Anders Svensson [a], Bo M. Vinther [a]

[a] Centre for Ice and Climate, Niels Bohr Institute, University of Copenhagen, Denmark
[b] Department of Geography, College of Science, Swansea University, Wales, UK
[c] Climate and Environmental Physics, Physics Institute, University of Bern, Switzerland
[d] Oeschger Centre for Climate Change Research, University of Bern, Bern, Switzerland
[e] College of Earth, Ocean, and Atmospheric Sciences, Oregon State University, USA
[f] Laboratoire des Sciences du Climat et de l'Environnement, UMR CEA/CNRS/UVSQ, Gif sur Yvette, France
[g] Scripps Institution of Oceanography, University of California, San Diego, USA

ARTICLE INFO

Article history:
Received 15 February 2014
Received in revised form
1 October 2014
Accepted 29 October 2014
Available online 26 November 2014

Keywords:
Paleoclimate
Greenland ice cores
GICC05 chronology
Tephra isochrons
Regional climate
Water isotopes ($\delta^{18}O$)
Heinrich event

ABSTRACT

We present a synchronization of the NGRIP, GRIP and GISP2 ice cores onto a master chronology extending back to 104 ka before present, providing a consistent chronological framework for these three Greenland records. The synchronization aligns distinct peaks in volcanic proxy records and other impurity records (chemo-stratigraphic matching) and assumes that these layers of elevated impurity content represent the same, instantaneous event in the past at all three sites. More than 900 marker horizons between the three cores have been identified and our matching is independently confirmed by 24 new and previously identified volcanic ash (tephra) tie-points. Using the reference horizons, we transfer the widely used Greenland ice-core chronology, GICC05modelext, to the two Summit cores, GRIP and GISP2. Furthermore, we provide gas chronologies for the Summit cores that are consistent with the GICC05modelext timescale by utilizing both existing and new gas data (CH_4 concentration and $\delta^{15}N$ of N_2). We infer that the accumulation contrast between the stadial and interstadial phases of the glacial period was ~10% greater at Summit compared to at NGRIP. The $\delta^{18}O$ temperature-proxy records from NGRIP, GRIP, and GISP2 are generally very similar and display synchronous behaviour at climate transitions. The $\delta^{18}O$ differences between Summit and NGRIP, however, changed slowly over the Last Glacial–Interglacial cycle and also underwent abrupt millennial-to-centennial-scale variations. We suggest that this observed latitudinal $\delta^{18}O$ gradient in Greenland during the glacial period is the result of 1) relatively higher degree of precipitation with a Pacific signature at NGRIP, 2) increased summer bias in precipitation at Summit, and 3) enhanced Rayleigh distillation due to an increased source-to-site distance and a potentially larger source-to-site temperature gradient. We propose that these processes are governed by changes in the North American Ice Sheet (NAIS) volume and North Atlantic sea-ice extent and/or sea-surface temperatures (SST) on orbital timescales, and that changing sea-ice extent and SSTs are the driving mechanisms on shorter timescales. Finally, we observe that maxima in the Summit–NGRIP $\delta^{18}O$ difference are roughly coincident with prominent Heinrich events. This suggests that the climatic reorganization that takes place during stadials with Heinrich events, possibly driven by a southward expansion of sea ice and low SSTs in the North Atlantic, are recorded in the ice-core records.

* Corresponding author. Tel.: +45 35 32 05 51.
E-mail address: inger@gfy.ku.dk (I.K. Seierstad).
[1] Deceased.

http://dx.doi.org/10.1016/j.quascirev.2014.10.032
0277-3791/

1. Introduction

Greenland ice-core records share a strong and consistent expression of past climate events in the North Atlantic region, e.g. the millennial-scale climate oscillations during the glacial period known as Dansgaard–Oeschger (D–O) events (Rasmussen et al., 2014, and references therein). The records offer an outstanding time-resolution of past climate events (e.g. Steffensen et al., 2008), but lack a common chronology, and substantial differences are apparent between the available timescales (Southon, 2004; Rasmussen et al., 2006; Svensson et al., 2008; Obrochta et al., 2014). In order to compare the climate records from the different ice cores, a common approach has been to align the records according to the D–O events using the $\delta^{18}O$ temperature proxy, thereby assuming that the abrupt climate shifts represent synchronous events between the sites (e.g. Grootes et al., 1993; North Greenland Ice Core Project Members, 2004; Svensson et al., 2008; Obrochta et al., 2014). This approach, however, precludes a detailed comparison of the ice-core records, because the "abrupt" alignment points are often several millennia apart and also because the various climate shifts may be expressed differently between the cores and proxies, making it difficult to pinpoint the exact depths of the marker horizons. An alternative and well-established ice-core synchronization method is to match up common volcanic peaks in profiles of sulphate concentration ($[SO_4^{2-}]$), Electrical Conductivity Measurements (ECM), Di-electrical Profiling (DEP) and conductivity of melted ice (e.g. Taylor et al., 1993a; Clausen et al., 1997; Vinther et al., 2006; Rasmussen et al., 2008, 2013; Svensson et al., 2013). This volcanic matching method does not rely on a prior assumption of climatic synchroneity at the different sites, and can thus be used to test for potential leads and lags between the archives. Furthermore, volcanic matching presents a more accurate synchronization with more finely spaced tie-points (down to sub-annual resolution) that are formed by the effectively instantaneous deposition of volcanic material (Palmer et al., 2001; Rasmussen et al., 2008). Rasmussen et al. (2008) demonstrated that the density of match points could be increased even further by combining volcanic matching with the identification of common and distinct peaks in calcium ($[Ca^{2+}]$) and ammonium profiles ($[NH_4^+]$), interpreted as major dust deposition and biomass burning events, respectively. Since this combined method relies on identifying stratigraphic markers in a range of chemistry records, we refer to this method as chemo-stratigraphic matching.

In recent years there has been a massive effort to link the Greenland ice cores by volcanic or chemo-stratigraphic matching (see references below) to establish a consistent chronological framework based on the most recent annual-layer-counted timescale, the Greenland Ice Core Chronology 2005 (GICC05) and its flow-model based extension, GICC05modelext (Andersen et al., 2006; Rasmussen et al., 2006; Svensson et al., 2006; Vinther et al., 2006; Svensson et al., 2008; Wolff et al., 2010). As yet, only two out of the four most recently drilled Greenland deep ice cores have been synchronized across their entire undisturbed sections, namely the NGRIP core and the NEEM core (Rasmussen et al., 2013). Only parts of the two other recent deep Greenland cores, the GRIP and the GISP2 cores (together denoted "the Summit cores" throughout this paper), have been synchronized to the GICC05-modelext timescale (Rasmussen et al., 2006; Vinther et al., 2006; Rasmussen et al., 2008; Blockley et al., 2012; Svensson et al., 2013).

Building on the existing partial synchronization of the GRIP, GISP2 and NGRIP cores, we extend the chemo-stratigraphic synchronization to the entire length of the stratigraphically undisturbed sections of the two Summit cores, and present the records on the GICC05modelext timescale back to 104 thousand years before 2000 CE (ka b2k). Independent data in the form of new and existing volcanic ash marker horizons (tephra isochrons) are used to validate the chemo-stratigraphic matching, and to complement it in sections without chemo-stratigraphic match points. In order to create a consistent chronological framework for both the ice and gas phase of the three cores, we also provide gas chronologies for the GRIP and GISP2 cores that are consistent with the GICC05modelext timescale by calculating the ice age–gas age difference (Δage; Schwander and Stauffer, 1984) constrained by both new and existing measurements of CH_4 concentration and $\delta^{15}N$ of N_2.

The benefits of having a tight synchronization of the Greenland ice cores are numerous. For instance, Greenland composite data records can be constructed from two or several cores in cases where data are not available for the entire length of each core (e.g. Elsässer et al., 2014). Furthermore, the reference horizons can provide ages and serve as ground truth when tracking radar layers on radio echograms between ice-coring sites (Karlsson et al., 2013; Panton, 2014) and the horizons can potentially constrain models describing the past conditions of the Greenland Ice Sheet (GIS). Finally, a consistent chronological framework for the network of Greenland deep ice cores allows an estimation of past elevation changes of the ice sheet (Vinther et al., 2009; NEEM Community Members, 2013) and gives insight into past regional climate variability and dynamics in much greater detail than previously attained (Langen and Vinther, 2009; Guillevic et al., 2013; Buizert et al., 2014).

In this paper, the resulting match points are used to make a detailed comparison between the GICC05modelext chronology and another widely used annual-layer-counted chronology for Greenland ice cores, the GISP2 timescale (also known as the Meese/Sowers timescale; Alley et al., 1997; Meese et al., 1997). The match points also provide an assessment of the degree to which the climate records preserved in the GRIP, GISP2 and NGRIP ice cores share a common climate signal and reveal any regional differences. In particular, we investigate in detail previously reported differences between the glacial $\delta^{18}O$ levels recorded in the three synchronized ice cores (Johnsen et al., 2001; North Greenland Ice Core Project members, 2004). We discuss possible causes for the observed $\delta^{18}O$ differences and sketch a potential association between $\delta^{18}O$ features and climate conditions prevailing at the time of Heinrich (H) events identified in North Atlantic deep sea sediments and arising from major ice-rafting events (Ruddiman, 1977; Heinrich, 1988; Bond et al., 1992; Broecker et al., 1992; Hemming, 2004).

2. Data and methods

2.1. Chemo-stratigraphic matching

2.1.1. Identification of common events

Following the approach of Rasmussen et al. (2008), distinct peaks in the impurity records of NGRIP, GRIP, and GISP2 have been matched, based on the assumption that prominent layers with elevated impurity content represent the same, instantaneous event at all three sites. An example of the matching is shown in Fig. 1, which displays an 1107-year-long section around 59 ka b2k. Most of the matched events are of volcanic origin, expressed as peaks in sulphate and in the profiles of ECM, DEP, and conductivity of the liquid phase (Taylor et al., 1993a; Moore et al., 1994; Clausen et al., 1997; Mayewski et al., 1997; Taylor et al., 1997; Wolff et al., 1997; Dahl-Jensen et al., 2002; Bigler, 2004; Plummer et al., 2012; Rasmussen et al., 2013). Volcanic match points are supplemented by a few exceptionally large peaks in calcium and ammonium and by common patterns of ammonium peaks (Fuhrer et al., 1993, 1996; Taylor et al., 1996; Mayewski et al., 1997; Bigler, 2004; Rasmussen et al., 2008). In some cases prominent dips in the ECM records

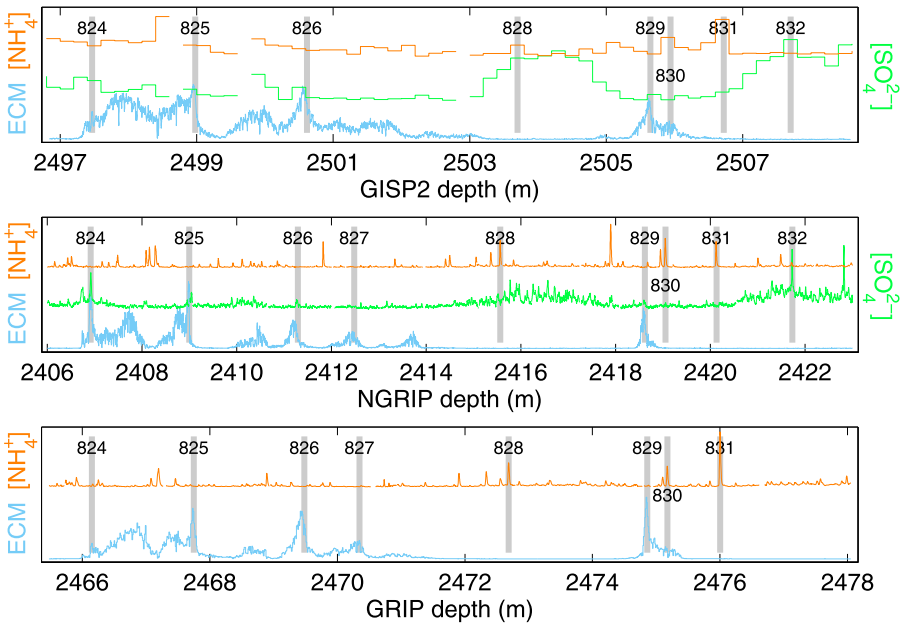

Fig. 1. Example of chemo-stratigraphic matching between the GISP2 (top), NGRIP (middle) and GRIP (bottom) cores for the period 58.56–59.67 ka b2k (covering the end of GS-18, GI-17.2, GS-17.2 and GI-17.1; Rasmussen et al., 2014). Match points (grey bars) no. 824–827, 829 and 832 are identified from ECM (blue) and/or sulphate (green) records and interpreted as volcanic events, while match points 828, 830 and 831 are identified from the ammonium record (orange) and thought to originate from biomass burning. Match point 827 links GRIP and NGRIP only, since this event has not been recorded in the GISP2 ECM signal or in any of the sulphate profiles. The uncertainty on the exact position of match point 827 is greater than for the other ECM match points displayed in the figure due to the broad nature of this ECM peak. Ammonium match point 830 and 831 are located right next to an ECM-based match point, and we consider the combined pattern formed by points 829–831 very reliable, while match point 828 is less certain due to the greater distance to neighbouring match points. Finally, match point 832 is a GISP2–NGRIP sulphate-based match point (there are no available GRIP sulphate data across this interval), with no clearly associated ECM-peak. DEP records (not shown) from the NGRIP and GRIP cores have been used in parallel with the other records when performing the matching, and generally show the same events as the ECM signal. Calcium is not shown because there are no calcium-based match points in this section. See text for data references. Since the absolute values are of no importance for the matching, units and values have been omitted from the *y*-axis for clarity.

(typically due to elevated ammonium loading (Moore et al., 1994)), have been used to either match up the cores or to adjust the depth assignment of a particular match point derived from one of the other parameters mentioned above. Note that the scale of the records in Fig. 1 is very compressed, so that not every feature is as easily visible as when the matching was performed using a dedicated software tool ("Matchmaker"; can be obtained from S. O. Rasmussen upon request). For example, the ECM-based match point 825 is supported by a similar pattern of ammonium peaks in NGRIP and GRIP, and the exact depth position of the ammonium-based match point 831 in GISP2 is determined by a well-defined dip in the ECM, giving rise to a much more precise depth assignment than possible from the low-resolution GISP2 ammonium data alone.

2.1.2. Chemo-stratigraphic match points

The resulting match points (Figs. 2 and 8) represent coeval horizons of age a_i between the cores, specified by depths (d_i) in one core and depths (D_i) in another core, where the subscript i denotes match-point number, starting with $i = 1$ at the youngest match point. In order to evaluate the matching throughout the matching process we use the method outlined by Rasmussen et al. (2008, 2013) where we expect the depth difference ($d_i - D_i$) curve to be smooth in sections with stable climatic conditions, and the ratio of the mean layer thicknesses between two cores, $r_i = (d_i - d_{i-1})/(D_i - D_{i-1})$, only to change abruptly at climate transitions (reflecting changing accumulation gradients) or when neighbouring match points are found very close to each other (reflecting that the ratio r_i is sensitive to the exact location of densely spaced match points). For all sections, 2–3 investigators have done the matching independently with repeated inspections to test the reproducibility of the matching. The published match points are the common agreement between all investigators and are available from www.icecores.dk/data. There are 783 chemo-stratigraphic match points that are common to all three cores with a further 150 chemo-stratigraphic links between two of the cores. These numbers include the previously published match points in the sections 14.9–32.45 ka b2k (Rasmussen et al., 2008), 32.45–48 ka b2k (GRIP and NGRIP only; Blockley et al., 2012), and 74.0–76.0 ka b2k (Svensson et al., 2013). Uncertainty estimates on the matching method is adopted from Rasmussen et al. (2008, 2013) and are evaluated in Section 2.4.

2.1.3. Revision of previously published ECM-based match points

Between 8.2 ka and 14.9 ka b2k the ECM-based NGRIP–-GRIP–GISP2 match points published by Rasmussen et al. (2006) have been updated. Several investigators have re-examined this section with all available chemistry data using the Matchmaker tool. As a result of this revision, the number of match points across this section has increased by a factor of seven, and some adjustment of the synchronization has been introduced. The adjustment between the cores is typically of the order of 5 cm or less, but grows to around 20 cm in a few cases, and reaches a maximum of 33 cm in Greenland Interstadial (GI) 1.

2.1.4. Density of match points

The average depth spacing between neighbouring match points is 3.4 m, corresponding to an average duration between match points of 125 years (calculated from common match points between sets of two cores). However, the spacing of match points varies significantly down the cores, ranging from less than 0.1 m to nearly 80 m. This corresponds to a time resolution from subannual

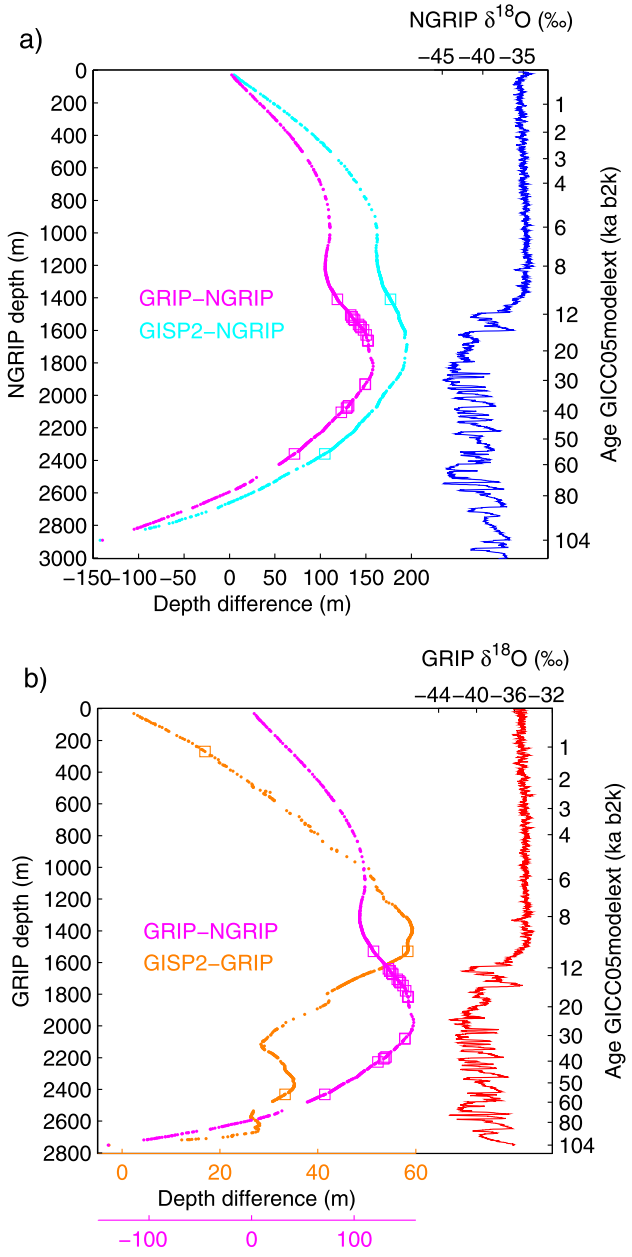

Fig. 2. Match points displayed on the NGRIP depth scale (a) and GRIP depth scale (b) vs. differences in depths of coeval horizons. a) Bottom axis: GRIP–NGRIP (magenta) and GISP2–NGRIP (cyan) depth differences based on chemo-stratigraphic match points (dots) and tephra tie-points (squares). Top axis: NGRIP $\delta^{18}O$ with 5.5 m moving-average smoothing applied (blue). GICC05modelext ages are shown on the right axis. b) Same caption as for a) except that the depth differences are GRIP–NGRIP (magenta) and GISP2–GRIP (orange) and that the $\delta^{18}O$ profile is from GRIP (red). Note that the range of GRIP–NGRIP depths differences is about five times greater than the GISP2–GRIP range.

to 10 ky. The distribution of match points in the cores depends on the existence of common instantaneous depositional events in the past, the expression of the events in the measured data profiles, the availability and the resolution of data for each section and core, and the varying degree of background impurity levels (which depends on the background climate). In general, the highest temporal density of match points is found in relatively warm climate periods. For instance, 48% of the matched events are identified in the Holocene section even though this time interval takes up only 11% of the entire synchronized section. Similarly, in the glacial section, 79% of the matched events are found in interstadials, although interstadials comprise only about half of the glacial period. The main explanation for this imbalance is the elevated impurity loading during the stadials: high dust concentration during stadials causes the ECM and DEP signals to be significantly muted, so that none or only the strongest volcanic peaks are identifiable (see sections around match points 828 and 832 in Fig. 1 and e.g. Taylor et al., 1993b). Also, the background [SO_4^{2-}], [Ca^{2+}], and [NH_4^+] levels are elevated during stadials, and single peaks from e.g. volcanic eruptions, biomass burning, and dust storms stand out less clearly in the data profiles. The difference in signal-to-noise ratio between stadials and interstadials is clearly reflected by the average time separation between neighbouring match points of 29 years in the Holocene, 139 years in interstadials, and 501 years in stadials. Gaps in the match points of one to two millennia are common in the stadial intervals. Here, tephra marker horizons are an important complement to chemo-stratigraphic matching.

2.2. Tephra marker horizons

Volcanic ash deposited on the Greenland Ice Sheet can be traced as isochrons between different ice cores if the glass shards originate from the same eruption and thus carry the same geochemical characteristics. Most of the volcanic ash deposits identified are not visible to the naked eye in the ice cores because of a low concentration of particles and/or small shard sizes and are referred to as cryptotephra deposits. Over the last few years there has been an intensified focus on the search for cryptotephra in Greenland ice (Mortensen et al., 2005; Davies et al., 2010, 2014; Abbott et al., 2012; Coulter et al., 2012; Bourne et al., 2013, in press) and recent work demonstrates the huge potential of establishing isochrons between the deep ice-core records (Rasmussen et al., 2013). However, only the Saksunarvatn Ash and the North Atlantic Ash Zone 2 (NAAZ II; Z2) can be traced between all three ice cores studied here, while the Settlement Layer is found in the two Summit cores, and the Vedde Ash has been identified in GRIP and NGRIP (See Table S1 in supplementary material; Grönvold et al., 1995; Ram et al., 1996; Zielinski et al., 1997; Mortensen et al., 2005; Svensson et al., 2008). Together with the parallel study of Bourne et al. (in press) we report 20 new tephra correlations between GRIP and NGRIP. Thus, in total, 24 tephra tie-points are used in our study.

2.2.1. New tephra isochrons between NGRIP and GRIP

Detailed investigation of ice spanning selected intervals between 12.5 ka and 45 ka b2k reveal 20 new tephra isochrons between GRIP and NGRIP located within GI-1 and GI-8, and in Greenland Stadial (GS) 1, 2.1, 5.2, 9 and 10 (following the stratigraphic nomenclature of Rasmussen et al., 2014). Initial work focused on NGRIP, and ice samples were selected according to the position of sulphate peaks, rapid climatic transitions and the age estimates of well-known volcanic eruptions. Fewer samples were investigated from GRIP and the sampling was largely guided by the search for well-known eruptions yet to be traced in Greenland ice cores (e.g. the Laacher See and Campanian Ignimbrite) and the position of tephra horizons identified in NEEM (Rasmussen et al., 2013). See Table S1 and Bourne et al. (in press) for details on the sample preparation and the electron-probe micro analysis of the volcanic glass shards.

Fifteen of the 20 new tephra isochrons are identified close to a chemo-stratigraphic match point (Fig. 3). Iceland is the dominant source with seven tholeiitic basaltic horizons (Fig. 3A), six transitional alkali horizons (Fig. 3B) and two rhyolitic horizons attributed to this source (Fig. 3C). Although there is a small element of scatter in some populations, the overlapping geochemical envelopes

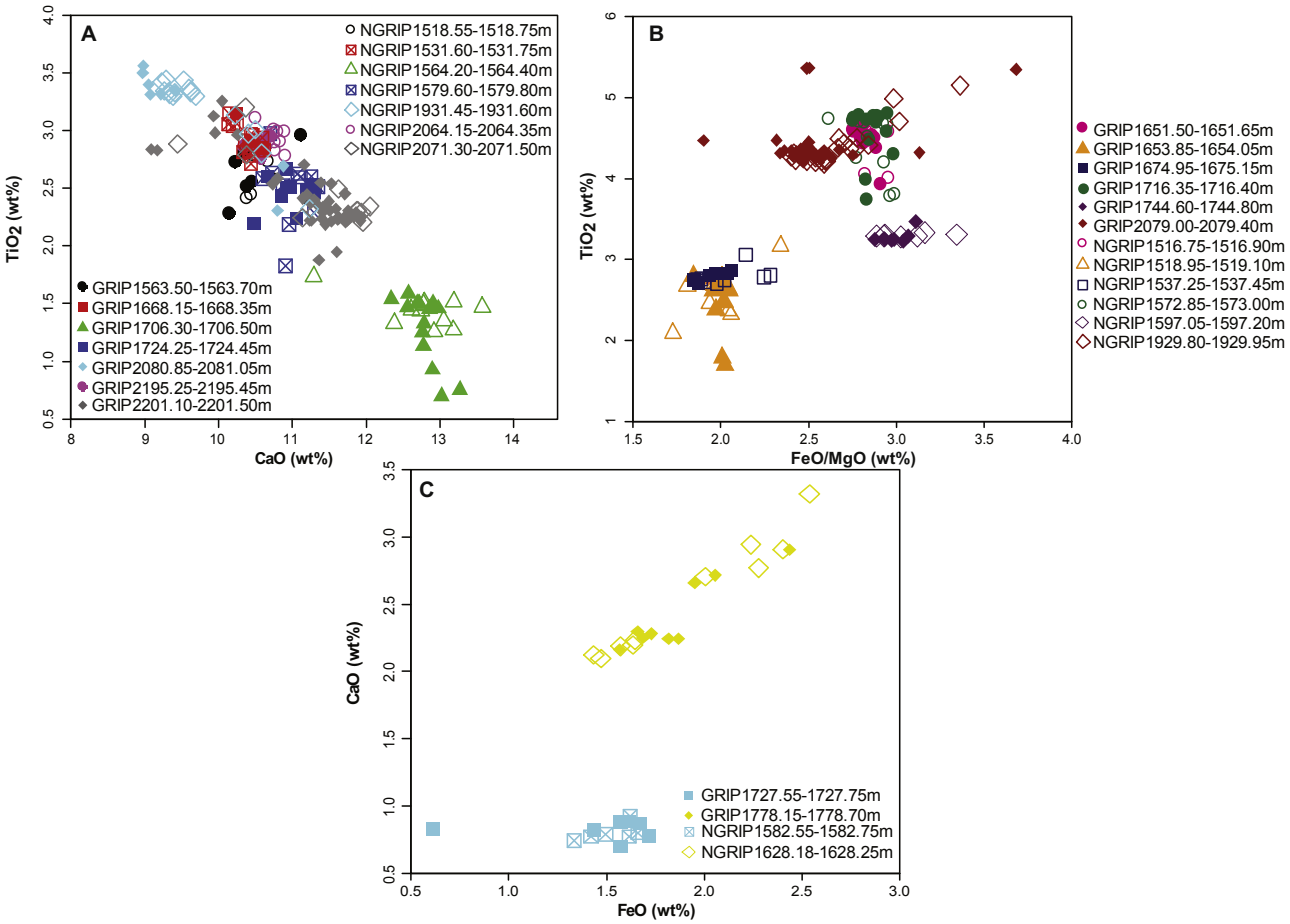

Fig. 3. Biplots showing new tephra tie-points that support and validate the chemo-stratigraphic matching between NGRIP and GRIP. Glass shard analyses from GRIP deposits are represented by filled symbols and those from NGRIP are represented by open symbols. Same colour and shape symbol are used for correlative deposits. Major element data are normalised to 100%. A) Biplot of CaO vs TiO_2 to highlight tholeiitic basalt tie-points. B) Biplot of FeO/MgO vs TiO_2 to highlight transitional alkali basalt tie-points. C) Biplot of FeO vs CaO to highlight rhyolitic tie-points.

support the correlation of tephras between the two ice cores. Similarity coefficients and statistical distance tests also support these correlations (see Table S1 and Bourne et al. (in press) for further details). Five of the new tephra tie-points are located in sections where no chemo-stratigraphic match points have been identified nearby, and allow a refinement of the previously published chemo-stratigraphic synchronization (Rasmussen et al., 2008; Blockley et al., 2012). These five tephra horizons fill gaps in the match points during GS-2.1 (three tie-points), GS-9 and GS-10, respectively. They have been used for timescale transfer in a similar way as described by Rasmussen et al. (2013), using the middle depth of the tephra sample. Three are rhyolitic in composition (Fig. 4A, B) and two have a tholeiitic basalt composition (Fig. 4C, D).

2.3. Synchronization and application of the GICC05 and GICC05modelext chronologies to the GRIP and GISP2 cores

The depth–depth relationship acquired from the 933 chemo-stratigraphic match points and the 5 tephra match points, allows GICC05 and GICC05modelext to be transferred to the full length of the undisturbed sections of the GRIP and GISP2 cores, and thus to synchronize the ice-core records on a master chronology for Greenland. Below we describe the GICC05 and GICC05modelext chronologies and the timescale transfer to GRIP and GISP2, as well as the resampling procedure of $\delta^{18}O$ data from the cores. Subsequently, we use the chemo-stratigraphic match points to evaluate the uncertainty estimate of the Holocene part of GICC05.

2.3.1. The GICC05 and GICC05modelext chronologies

The Holocene part (0–11.7 ka) of the GICC05 timescale exists at an annual resolution for the DYE-3, GRIP and NGRIP ice cores (Rasmussen et al., 2006; Vinther et al., 2006). This part of the timescale was constructed in such a way that the core(s) showing the optimal annual stratification across a specific age interval was chosen as the leading core(s) for the annual layer counting. All cores were linked through coeval peaks in ECM, and in between these common ECM peaks the number of identified annual layers in the leading core(s) was transferred to the non-leading core(s). Supplemental counting was carried out on the non-leading core(s) with less clear annual cycles, and this supplemental counting was used as a guide to assign the most likely annual layer thickness distribution in the non-leading core. The glacial section of GICC05 is based on annual layer identification in the NGRIP core solely, utilising a multi-parameter high-resolution dataset (Andersen et al., 2006; Rasmussen et al., 2006; Svensson et al., 2006, 2008). Beyond 60.2 ka, where the NGRIP annual layers become too thin for reliable identification using existing data, the chronology has been extended by a flow-model-based timescale, which is available in 20-yr resolution, and the combined timescale is named GICC05modelext (Wolff et al., 2010). The uncertainty on the annual-layer-counted timescale is specified by the Maximum Counting Error

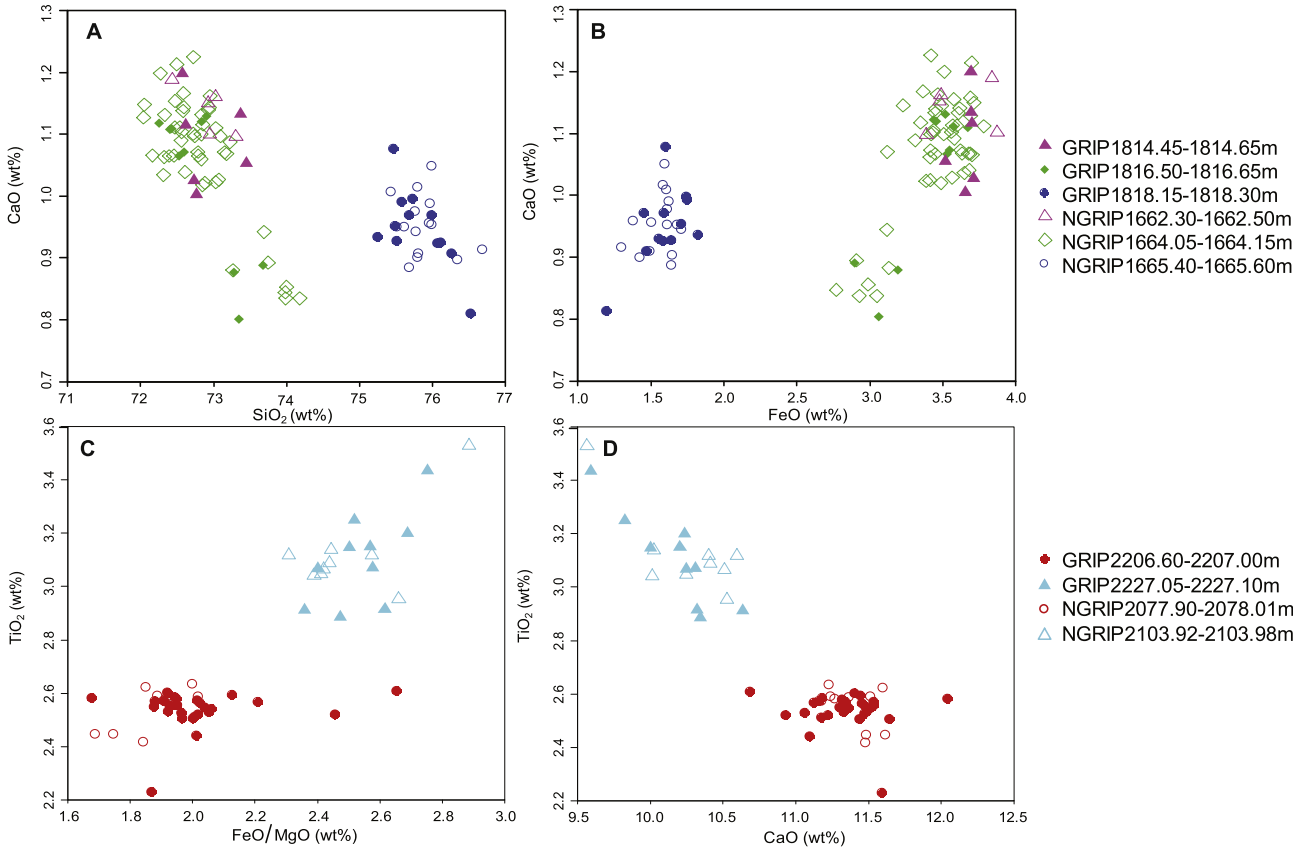

Fig. 4. Biplots showing new tephra tie-points that fill gaps in the matching of NGRIP and GRIP and are used for timescale transfer. Glass shards from GRIP deposits are represented by filled symbols and those for NGRIP are represented by open symbols. Same colour and shape symbol are used for correlative deposits. Major element data are normalised to 100%. Biplots of: A) SiO_2 vs CaO and B) FeO vs CaO for three rhyolitic tie-points. Biplots of: C) FeO/MgO vs TiO_2 and D) CaO vs TiO_2 for two tholeiitic basalt tie-points.

(MCE) which is an accumulated error, obtained by adding ½ year to both the age of the ice and the MCE each time an uncertain layer is encountered.

2.3.2. *Transfer of GICC05modelext to GRIP and GISP2 and resampling of $\delta^{18}O$ data*

A depth–age scale accompanies this paper for GRIP and GISP2 over the interval 0–104 ka b2k in steps of 20 years on GICC05modelext together with previously published $\delta^{18}O$ data (Grootes and Stuiver, 1997; Johnsen et al., 1997; Stuiver and Grootes, 2000). The GICC05 timescale is already available for GRIP in the Holocene, while GICC05 is transferred from NGRIP to GRIP in the glacial section by linear interpolation in depth–depth space as follows: NGRIP depths corresponding to 20-yr intervals have been obtained from the NGRIP GICC05 annual-layer-counted chronology (and from GICC05modelext beyond 60.2 ka b2k). The corresponding GRIP depths were then obtained by linear interpolation between the NGRIP–GRIP match-point depths, thereby assuming that the ratio of the mean annual layer thickness of the two cores remains constant between common match points. By this approach, the annual layer thickness variability between match points is transferred from NGRIP to GRIP. In a similar way, for the GISP2 core, we have transferred the Holocene part of GICC05 from the GRIP core due to the geographical proximity of the two sites, while the glacial part of the timescale has been transferred from NGRIP. The GRIP and GISP2 $\delta^{18}O$ data sets on GICC05modelext are displayed along with NGRIP $\delta^{18}O$ (North Greenland Ice Core Project Members, 2004) in 200-yr resolution in Fig. 8, and the glacial section can be viewed in 20-yr resolution in Fig. 1 of Rasmussen et al. (2014). For GRIP, a depth–age scale in steps of 0.55 cm (the so-called "bag" length) with corresponding $\delta^{18}O$ in bag mean values from detailed $\delta^{18}O$ data measured at Centre for Ice and Climate in Copenhagen is also provided (Johnsen et al., 1997). Again, the timescale was transferred in depth space by converting GRIP depths for each bag to NGRIP depths by linear interpolation between match-point depths, and obtaining ages from the NGRIP depth–age relation. For GISP2 we supply a GICC05modelext-consistent timescale to be used with the publicly available GISP2 impurity data (Mayewski et al., 1997).

2.3.3. *Evaluation of the GICC05 timescale in the Holocene*

The new chemo-stratigraphic match points are employed to evaluate the existing ECM-based synchronization of the three cores constituting the Holocene section of the GICC05 timescale. We compare the NGRIP–GRIP match points with the depth–depth relationship for NGRIP and GRIP from the annually resolved GICC05 timescale. Back to 1.8 ka b2k, where data from GRIP, NGRIP and DYE-3 have been used in parallel to construct GICC05, our match points and the depth–depth relationship from GICC05 agree within one year, which is equivalent to the estimated potential mismatch between ECM peaks in GICC05 for this section (Vinther et al., 2006). A similar good agreement between GICC05 and the NGRIP–GRIP match points is seen in the oldest part where the main annual layer counting is performed on NGRIP high-resolution data (10.3–11.7 ka b2k) and where the NGRIP ECM and GRIP ECM records show the strongest correlation and variance (Vinther et al., 2006). In the intermediate time section (1.8–10.3 ka b2k), where the annual layer counting relies mainly on DYE-3 and GRIP data, the GICC05 depth relationship and our match points typically agree within 1–2 years, which is within the estimated uncertainty.

However, in four cases (around 5.94, 8.26, 8.97 and 9.60 ka b2k) there is an offset of 3–4 years between our match points and GICC05, which is at or slightly above the estimated mismatch within matched sections of GICC05, and at 4.26 ka the offset between the two different data synchronizations reaches a maximum of 9 years. We believe that the observed offsets between the chemo-stratigraphic match points and the GICC05 parallel dating most likely are related to the transfer of the annual layer counts from the leading core(s) to the non-leading core(s) in GICC05 in intervals where the clear ECM peaks are sparse. The chemo-stratigraphic matching is able to identify more clear match points and we therefore believe that the difference is caused by the availability of more match points between the cores. We consider the observed inconsistencies in the Holocene to be negligible for our work and too small to justify a revision of the GICC05 timescale. For the Holocene section of GICC05 we recommend that a synchronization uncertainty of a few years should be added on top of the existing MCE to the non-leading cores. As outlined above, the synchronization uncertainty is probably higher in a few depth intervals, especially where the matching is performed on sections from the brittle ice zone.

2.4. Validation and uncertainty

2.4.1. Validation of the chemo-stratigraphic matching method and evaluation of general uncertainty estimates

The 24 tephra layers that unambiguously correlate geochemically between all or two of the ice cores can be used to test the chemo-stratigraphic matching and to evaluate the estimated uncertainty on the matching and interpolation method reported by Rasmussen et al. (2008, 2013). All tephra isochrons are consistent within uncertainties with our match points or the linear interpolation curve in between match points (Fig. 2).

Rasmussen et al. (2008) estimated the precision of the chemo-stratigraphic matching (σ_{mp}) to typically 10 cm (1σ) or less. In cases of less well-defined peaks the matching offset was estimated to be slightly higher, and in cases where match points were based on the low resolution GISP2 [SO_4^{2-}] and [NH_4^+] data alone, the uncertainty was set to 20 cm, corresponding to the resolution of the GISP2 ion concentration data. The maximum synchronization offset in the sections where the timescale was transferred by linear interpolation (σ_{interp}) was estimated to 0.5 m, except across an unusually long match-point gap across GS-2.1. The chemo-stratigraphic match points are by their nature defined as points in a depth–depth diagram, while the tephra tie-points span an area defined by the sample length, *L*, of the two correlative layers. The length of the tephra samples used in this study is 16 cm on average, varying from 1 mm (where visible horizons are identified) to 55 cm, dependent on the actual span of the tephra horizon and the ice sampling resolution. For cryptotephra layers, the entire interval *L* is interpreted as the uncertainty band on the location of the volcanic ash horizon. Eight tephra isochrons with small sampling intervals (<10 cm) in both cores show a compelling agreement with the chemo-stratigraphic match points, and suggest that $\sigma_{mp} = 10$ cm is a conservative uncertainty estimate on the match points. Based on the evidence provided by the 24 tephra tie-points we conclude that the general uncertainty estimates on the matching and interpolation method given by Rasmussen et al. (2008, 2013) are realistic and probably conservative.

2.4.2. Sections with higher uncertainty on the synchronization

The varying density of match points (Section 2.1.4) means that the uncertainty on the timescale transfer to GRIP and GISP2 varies. In the following, sections where the synchronization uncertainty σ_{interp} is considered to be greater than the general estimate of 0.5 m (Rasmussen et al., 2008) are discussed. The longest gap between neighbouring match points appears in the GRIP core during the time period covering GS-19.1, GI-18 and GS-18. The gap is nearly 10 ky long, corresponding to 80 m and 55 m on the NGRIP and GRIP depth scales, respectively. Most of the match points between NGRIP and GISP2 in the same time period are identified in the sulphate records, which is not available for GRIP in this depth interval. We estimate that the maximum uncertainty for GRIP across this section is about 1 m (up to 250 years). Looking at the resampled GRIP data on GICC05modelext (Figs. 8 and 1 from Rasmussen et al. (2014)) the transitions of $\delta^{18}O$ and [Ca^{2+}] into and out of GI-18 in the GRIP record seem to be offset by 20–40 years relative to the NGRIP and GISP2 records, indicating that the synchronization error is likely to be smaller than the estimated maximum of 1 m. Across GS-2.1 we maintain the synchronization uncertainty estimate of 1 m (about 60 years) from Rasmussen et al. (2008), except for between NGRIP and GRIP in the youngest half of GS-2.1, where we believe that the synchronization offset is down to 0.5 m (less than 30 years) since three new tephra horizons between NGRIP and GRIP are providing a more smooth (and glaciologically plausible) depth difference curve across the chemo-stratigraphic match-point gap. In the Holocene section, we observe a varying density of match points with age. The section between 2.7 ka and 7.2 ka b2k stands out as having the lowest temporal and spatial Holocene density of match points, where the distance between neighbouring match points in several cases exceeds 40 m (up to nearly 360 years), and reaches a maximum distance of slightly more than 60 m at 3.0 ka b2k. Across these long gaps we estimate that the synchronization uncertainty may be up to 1.5 m (or 15 years). We ascribe the low density of match points in this section to fewer available data series across the brittle zones, which in total span the period 2.9–8.8 ka b2k in the three cores (Gow et al., 1997; Vinther et al., 2006). Across the brittle zones we also observe a high degree of inter-core variability in the layer thickness, especially between GISP2 and each of the two other cores. The relative changes in layer thickness may be real or may be artificial due to reduced depth control across the brittle zones. The highest temporal density of match points in the Holocene is observed in the section older than ~8 ka, which is characterized by a combination of good data coverage and higher volcanic activity following the glacial-interglacial transition (Huybers and Langmuir, 2009).

The deepest match point at 104 ka (GISP2: 2748.82 m, GRIP: 2751.50 m, NGRIP: 2891.26 m) differs from the rest of the match points by being defined by a climate transition, i.e. the midpoint in the transition in $\delta^{18}O$ between GS-23.2 and GI-23.1. We employ this approach because there are no reliable candidates for a chemo-stratigraphic match in this section, and we estimate the uncertainty σ_{mp} on this particular match point to 0.5 m. However, we acknowledge that there is a risk that the abrupt change in $\delta^{18}O$ in the GISP2 and/or GRIP records may not represent the transition between GS-23.2 and GI-23.1, but could be the result of stratigraphic distortion due to near-bedrock flow deformation. Indeed, the $\delta^{18}O$ curves become fundamentally different just below this match point as previously reported by Grootes et al. (1993), and higher variability in GISP2 and GRIP layer thickness is observed in GI-23.1 compared to what we would expect from the relatively flat $\delta^{18}O$ curves (Fig. 7a, b). In particular, there is a prominent positive anomaly in the GISP2 annual layer thickness around 90–95 ka b2k on an otherwise general trend of rapidly declining thicknesses beyond ~87 ka b2k. We are confident that the sequence of all D–O cycles in the Summit cores are preserved at least back to GI-22 (90.0 ka b2k; GISP2: ~2704 m; GRIP: ~2679 m) and most likely preserved back to the transition between GS-23.2 and GI-23.1 (Grootes et al., 1993; Taylor et al., 1993a; Landais et al., 2003; North Greenland Ice Core Project Members, 2004). Under all

circumstances we consider the potential synchronization error σ_{interp} in GI-23 to be about 1 m (maximum 500 years), partly due to the high variability in GISP2 and GRIP layer thicknesses in the youngest part of GI-23, and partly due to the 6 ky long match-point gap in the oldest part of GI-23.

2.5. GICC05modelext gas chronology for the GISP2 and GRIP cores

Here we describe the construction of a GICC05modelext gas chronology for GRIP and GISP2. Recently, GICC05modelext gas chronologies were published for NEEM (Rasmussen et al., 2013) and NGRIP (Kindler et al., 2014).

2.5.1. GISP2 gas chronology

The GISP2 gas chronology is constructed by subtracting the ice age–gas age difference (Δage) from the ice chronology. We estimate the present day Δage at GISP2 to be 190 years (Supplementary Material). For the deep core we reconstruct past Δage values using a coupled firn densification-heat diffusion model to simulate past firn column evolution and bubble closure, constrained by measurements of CH_4 and $\delta^{15}N$ of N_2 (Fig. 5). For CH_4 we use a compilation of published (Brook et al., 1996, 2000; Grachev et al., 2007; Brook and Severinghaus, 2011) and previously unpublished data from Oregon State University, using the solubility correction of Mitchell et al. (2011) where applicable. For $\delta^{15}N$ we use a compilation of published (Severinghaus et al., 1998; Severinghaus and Brook, 1999; Grachev et al., 2007; Kobashi et al., 2007, 2008a, 2008b; Orsi et al., 2014) and previously unpublished data from Scripps Institution of Oceanography. Older data from Bender et al. (1994) are excluded due to lower analytical precision. The $\delta^{15}N$ excursions caused by thermal diffusion in the firn column during abrupt climatic transitions provide the best possible constraint on Δage (Severinghaus et al., 1998; Leuenberger et al., 1999). For GISP2 reliable $\delta^{15}N$ data are available for the 8.2 ka event, the deglacial sequence, and for the onset of GI-2.2, 3, 4, 7, 8, 12, 17.1, 17.2, 19.2, 20, 21.1, and 21.2 (Fig. 5c). We force the model to fit the $\delta^{15}N$ data; the model can only fit these data correctly if it models the correct Δage.

For abrupt transitions where $\delta^{15}N$ data are not available, we obtain additional constraints from CH_4 which changes in phase with Greenland climate within 50 years (Brook et al., 1996; Rosen et al., 2014). For these transitions, Δage is found by taking the difference in ice age between the depths corresponding to the midpoint of the CH_4 and $\delta^{18}O$ transitions, and then adding 25 years to account for the small lag of CH_4 behind Greenland climate (Huber et al., 2006). An uncertainty to each Δage tie-point is assigned by taking the root sum square of: 1) the uncertainty in determining the midpoint in the CH_4 transition, given the available data resolution; 2) the uncertainty in determining the midpoint in the $\delta^{18}O$ transition, given the available data resolution; and 3) the uncertainty in the CH_4 lag, which we take to be 25 years (i.e. the CH_4 marker lags the $\delta^{18}O$ marker by 0–50 years). The uncertainty is 85 years on average.

The modelling approach used here is identical to the one used to derive the NEEM gas chronology (Rasmussen et al., 2013). Firn densification physics is described by a dynamical version of the Herron–Langway model (Herron and Langway, 1980) with ice

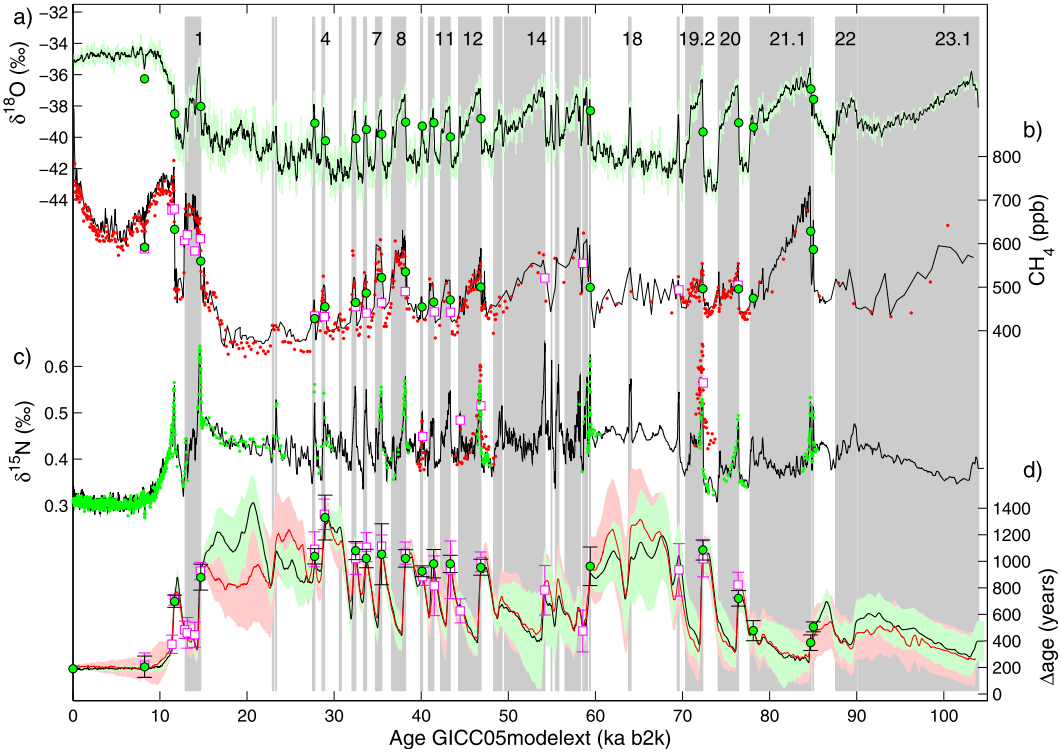

Fig. 5. GICC05modelext gas chronology and Δage for the GISP2 (black and green colours, circles) and GRIP (red and magenta colours, squares) cores. a) 20 year average GISP2 $\delta^{18}O$ of ice (green line) as a proxy for climate, with 7 point running mean (black line). b) Compilation of GISP2 CH_4 data (black line) and GRIP CH_4 data (red dots, Blunier and Brook (2001), Flückiger et al. (2004) and Landais et al. (2004)). c) Compilation of GISP2 $\delta^{15}N$ data (green dots) with model fit (black line), and GRIP $\delta^{15}N$ data (red dots, Lang et al. (1999) (GI-19.2 to GS-20); Landais et al. (2004) (GI-12 to GS-13) and Guillevic et al. (2013) (GI-9)). d) Empirical Δage constraints for GISP2 (green dots) and GRIP (magenta squares) are superimposed onto the modelled Δage curves with uncertainty envelope for GISP2 (black, green) and GRIP (red, pale red). The empirical Δage constraints have been deduced based on the identification of abrupt temperature changes recorded in the $\delta^{18}O$ (ice phase) and the $\delta^{15}N$ or CH_4 (gas phase) records for each ice core. The location of the GISP2 tie-points is indicated in the four records by similar symbols (green circles). GRIP tie-points (magenta squares) are indicated in the gas records only, but they have counterparts in the GRIP $\delta^{18}O$ record (not shown). Vertical grey bars represent interstadial conditions, and black numbers above the $\delta^{18}O$ profiles indicate selected Greenland Interstadials, as defined by Rasmussen et al. (2014). See text for more data references. See Supplementary Material regarding GISP2 and GRIP $\delta^{15}N$ offsets across GI-12, GS-13, GI-19.2 and GS-20.

thermal properties as described in Cuffey and Paterson (2010). We use a lock-in density $\rho_{lid} = \rho_{co} - 14$ kg m^{-3} (Schwander et al., 1997), with ρ_{co}, the temperature dependent close-off density, from Martinerie et al. (1994). Surface density and convective zone thickness are kept constant at $\rho_0 = 360$ kg m^{-3} (average density of Summit firn for the top 2 m (M. Albert et al., personal communication)) and 4 m (consistent with unpublished δ^{15}N measurements at Summit, and in line with other Greenland sites (Buizert et al., 2012)), respectively. The effect of dust on the densification process was included as described by Freitag et al. (2013) and Rasmussen et al. (2013). We use a depth resolution of 0.5 m down to the lower model domain at 1000 m depth, where we use a zero temperature gradient boundary condition. We use 2.5 and 0.5 year time steps for the densification and heat diffusion models, respectively, and track a firn layer down every 5 years. Δage is calculated by subtracting the gas age from the modelled ice age at lock-in (Buizert et al., 2013).

Model input consists of temperature (T) and accumulation (A) time series, both of which are poorly known back in time. The initial guess for T is derived from the δ^{18}O record, where we use a sensitivity of 0.55 and 0.33‰K^{-1} for the Holocene and glacial periods, respectively. The initial guess for A is the reconstructed accumulation history by Cuffey and Clow (1997) for 0–15.3 ka b2k, and $A = 76.5 \cdot \exp(0.17 \cdot \delta^{18}O)$ for 15.3–104 ka b2k. We allow the model to make adjustments to both input functions to optimize the fit to δ^{15}N and CH_4 constraints using an automated routine.

The final model fit to δ^{15}N data and CH_4 tie-points is shown in Fig. 5c, d. The RMS offset between model and observed δ^{15}N values is 0.013‰, compared to an analytical precision of 0.007‰. The RMS offset to the seven CH_4 tie-points for which we have no concomitant δ^{15}N data is 5 years; if we consider all 20 CH_4 tie-points, the RMS offset increases to 27 years. The uncertainty in Δage ($\sigma_{\Delta age}$) is estimated in the following way: at abrupt transitions where we have data constraints from either CH_4 or δ^{15}N, we set $\sigma_{\Delta age}$ to the uncertainty in the timing from that constraint. Between the tie-points we set $\sigma_{\Delta age}$ to the linearly interpolated uncertainty of the two adjacent tie-points plus $0.05 \cdot \Delta t$, with Δt being the distance to the nearest tie-point in years. The latter ensures that the uncertainty increases as we move away from the data constraints (Rasmussen et al., 2013). Beyond 90 ka b2k, $\sigma_{\Delta age}$ is kept constant. In the Holocene we let $\sigma_{\Delta age}$ increase linearly from 10 years (uncertainty in modern Δage) to 25 years at the 8.2 ka event (given by the uncertainty in δ^{15}N timing at 8.2 ka b2k) to 50 years at the onset of Holocene (given by the uncertainty in δ^{15}N timing at 11.7 ka b2k).

This ensures that the new GISP2 gas chronology is maximally consistent with the available timing constraints deduced from CH_4 and δ^{15}N data. There are four intervals during which we have no data constraints on Δage: 15–22, 48–59, 61–71 and 86–104 ka b2k. Further measurements are needed to refine the gas chronology during these intervals.

2.5.2. GRIP gas chronology

The GRIP gas age scale is constructed in a similar way as the GISP2 chronology. A modern Δage value of 210 years (Schwander et al., 1993) is used (see Supplementary material). To reconstruct the past GRIP Δage for the undisturbed part of the deep core, we use the Goujon firn densification model equipped with heat-diffusion (Goujon et al., 2003), as described in Rasmussen et al. (2013). This firn model is constrained by previously published δ^{15}N data and Δage tie-points defined using abrupt CH_4 transitions (Fig. 5), following the same procedure as for the GISP2 core. The reason for using two separate firn densification models for the GISP2 and the GRIP Δage evolution is that different authors (C. B. and M. G.) worked individually for purposes other than the presented work. For the current project, we use a consistent methodology to construct the gas chronology at both sites. Rasmussen et al. (2013) demonstrated that the model output from the two different firn models applied in our study agreed within uncertainties when constructing the NEEM gas chronology, corroborating that the GRIP and GISP2 Δage reconstructions are consistent despite the use of different firn densification models.

The temperature scenario (T) is a linear function of the GRIP δ^{18}O record (Johnsen et al., 1992) corrected for sea water isotopic composition (Jouzel et al., 2003), with $T = (\delta^{18}O + \beta)/\alpha$, where α and β are tuned as described below. To calculate an a priori accumulation rate, we use the thinning function from Johnsen et al. (2001), using a simple one-dimensional ice flow model, and the GRIP annual layer thickness according to the GICC05modelext chronology (this study). Temperature (i.e. α and β) and accumulation rate are manually adjusted over a time window corresponding to each D–O event (GS-(n + 1) and GI-(n)), hence the time window is varying. For each time window, the "best" α is found first, followed by β and the percentage of accumulation rate reduction (if needed). If unique solutions for α, β and the accumulation rate reduction are not able to match the measured δ^{15}N and Δage data, the D–O event is split into smaller time windows. The time window is then moved to the next D–O event.

Between tie-points, the gas age scale uncertainty is calculated as for the GISP2 ice core. From 71 m to 1354.06 m depth, the Δage uncertainty increases linearly from 7.5 years to 91 years. In the part older than the last Δage tie-point (in GI-20c), where the Δage uncertainty has reached ±200 years, it is arbitrarily kept constant and equal to this value. Due to the absence of gas data, the GRIP gas age scale is badly constrained for the section older than GI-12, except for the period GI-19.2 to GI-20.

The GISP2 and GRIP CH_4 and δ^{15}N compilations on the new GICC05modelext timescale are provided as Supplementary material.

3. Results and discussion

3.1. Comparison of two annual-layer-counted chronologies from Greenland; the GISP2 timescale (Meese/Sowers) and the GICC05 timescale

The GISP2 and GICC05 timescales agree very well on absolute ages back to approx. 40 ka b2k (Fig. 6a and Svensson et al., 2008), but we observe substantial disagreements between the annual layer thickness profiles obtained from the two chronologies (Fig. 6c, d). These disagreements imply that the two chronologies are discordant when looking at differential ages, e.g. duration estimates of past climatic phases. The GICC05 chronology gives a consistent positive correlation between annual layer thickness and δ^{18}O across the stadial–interstadial variations: the annual layer thickness generally doubles in an interstadial compared to the preceding stadial (Fig. 6b, c and Svensson et al., 2006). In contrast, when applying the GISP2 timescale, the layer thickness doubles in some interstadials (e.g. GI-1), while no stadial/interstadial contrast is observed over other D–O cycles (e.g. across GS-5.2 to GS-7, and across GI-9 to 10). Relative to GICC05, the GISP2 timescale overestimates the annual layer thickness in most of the stadials (Fig. 6c) and thus underestimates stadial duration by 15% on average. Similarly, interstadial durations are on average overestimated by 15%. However there is a pronounced spread with some interstadials (GI-3 and 6) about 60% longer, and some stadials 30–40% shorter (GS-10, 11, 12 and 13) relative to GICC05 (Fig. 6d). Thus, when studying D–O cycles and their timing, the choice of timescale may heavily influence the interpretation. Based on the observed inconsistencies in the δ^{18}O-layer thickness relationship from the GISP2 timescale, we speculate that the annual signal in the changeable visual stratigraphy data used for the GISP2 timescale

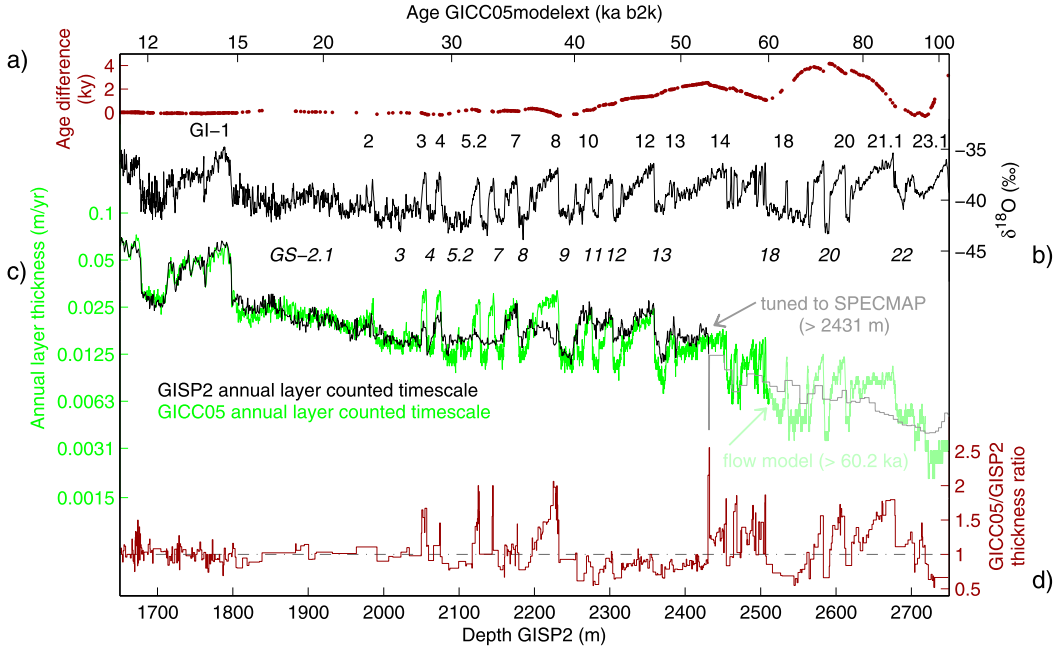

Fig. 6. Comparison of the glacial section of the GISP2 (Meese/Sowers) chronology and the GICC05modelext chronology. a) Age difference (GICC05modelext timescale − GISP2 timescale, dark red dots) at the depths of the match points b) GISP2 $\delta^{18}O$ on the GISP2 depth scale (bottom) with corresponding GICC05modelext ages (top). Selected GI numbers (black) and GS numbers (black italics) as defined by Rasmussen et al. (2014) are indicated. c) 20-yr average annual layer thickness for the GISP2 core obtained from the annual-layer-counted GISP2 (black) and GICC05 (green) timescales on a logarithmic axis. The arrows point out from where in the layer thickness profiles the timescales are modelled (>60.2 ka b2k, GICC05modelext, light green) or tuned to the SPECMAP timescale (>2431 m, GISP2 timescale, grey). The deeper sections are shown for completeness only and are not further discussed. d) The ratio of the mean annual layer thicknesses when using the GICC05modelext and GISP2 timescale, respectively (dark red).

(Alley et al., 1997) may have been misinterpreted in some sections. The typical overestimation of the stadial annual layer thickness in the GISP2 timescale indicates that the GISP2 visual stratigraphy was not fully able to resolve the thin (<~1.5 cm) annual layers during cold periods, while the underestimation of the annual layer thickness in some interstadials may be related to sub-annual variability in the GISP2 visible stratigraphy misidentified as annual layers (Alley et al., 1997; Andersen et al., 2006).

3.2. Annual layer thicknesses and past changes in relative accumulation rates

Fig. 7b displays the mean annual layer thickness, $\lambda_i = (d_i - d_{i-1})/(a_i - a_{i-1})$, between neighbouring match points for each core. The observed λ profiles are controlled by past accumulation rates and the accumulated strain since deposition. Modern day accumulation rates are 0.19 m ice equivalent per year (m.i.e./yr) at NGRIP, while GRIP and GISP2 receive 0.23 and 0.24 m.i.e./yr, respectively (Johnsen et al., 1992; Alley et al., 1993; Meese et al., 1997; North Greenland Ice Core Project Members, 2004). The differences in accumulation rate and strain histories are reflected in the ratios r_i of the layer thicknesses in one core to those of each of the other cores (defined in Section 2.1.2) which are displayed in Fig. 7c. The overall pattern is that NGRIP thicknesses with depth (or with age) slowly catch up with, and eventually overtake, layer thicknesses in the Summit cores. This is the result of faster thinning of layers with depth at Summit due to higher accumulation rates and no basal melt, while bottom melting conditions at NGRIP result in fairly constant layer thickness within both stadials and interstadials, respectively, in the deepest part of the NGRIP core.

Note that fully resolved GRIP (Holocene) and NGRIP layer thickness profiles are available from the annual layer counted chronology (Vinther et al., 2006; Svensson et al., 2008) and have been used for the timescale transfer described in Section 2.3.2 to produce detailed layer thickness profiles on the GICC05modelext timescale for the two Summit cores. Of the resulting detailed layer thickness profiles we show the glacial GISP2 section only (Fig. 6c). In Fig. 7b and in the text below we present only mean values between match points to allow consistent comparison.

3.2.1. Interstadial/stadial accumulation contrasts

Where the match-point density is sufficient to resolve the details, Fig. 7a, b show a strong positive correlation of all three λ profiles with the $\delta^{18}O$ profile across stadials and interstadials. A similar, albeit less systematic, pattern is observed in the GRIP/NGRIP and GISP2/NGRIP r values, which typically reach higher values during interstadials than in stadials (Fig. 7c). In other words, the interstadial/stadial accumulation contrast is larger for the two Summit cores than for NGRIP, suggesting spatially inhomogeneous changes in accumulation rates across D–O cycles. Where match-point density allows for a well-resolved λ profile (GI-1, 3, 4, 6, 7, 11, 12, 15.2, 19.2 and their preceding stadials), it is estimated that the Summit region on average experienced an approximately 10% higher stadial-to-interstadial accumulation increase compared to NGRIP. This difference can be explained by stronger accumulation response at Summit to ice-free conditions in the North Atlantic during interstadials, as suggested in a model study by Li et al. (2010), who found that GRIP had ~21% higher increase in accumulation compared to NGRIP when going from a stadial scenario to a sea-ice retreat scenario. Additionally, stronger winter drying during stadials at Summit compared to NGRIP due to less precipitation arriving from the Pacific may have contributed to the relatively thin stadial layers in the GRIP and GISP2 cores (Langen and Vinther, 2009). Indeed, accumulation rate reconstructions by Guillevic et al. (2013) show that the stadial–interstadial accumulation rate increase was nearly 9% higher at Summit compared to NGRIP going from GS-9 to GI-8, and nearly 5% from GS-11 to GI-10. The reconstructions across GS-10 to GI-9, however, are not as clear with similar accumulation increase for GISP2 and NGRIP, and a GRIP

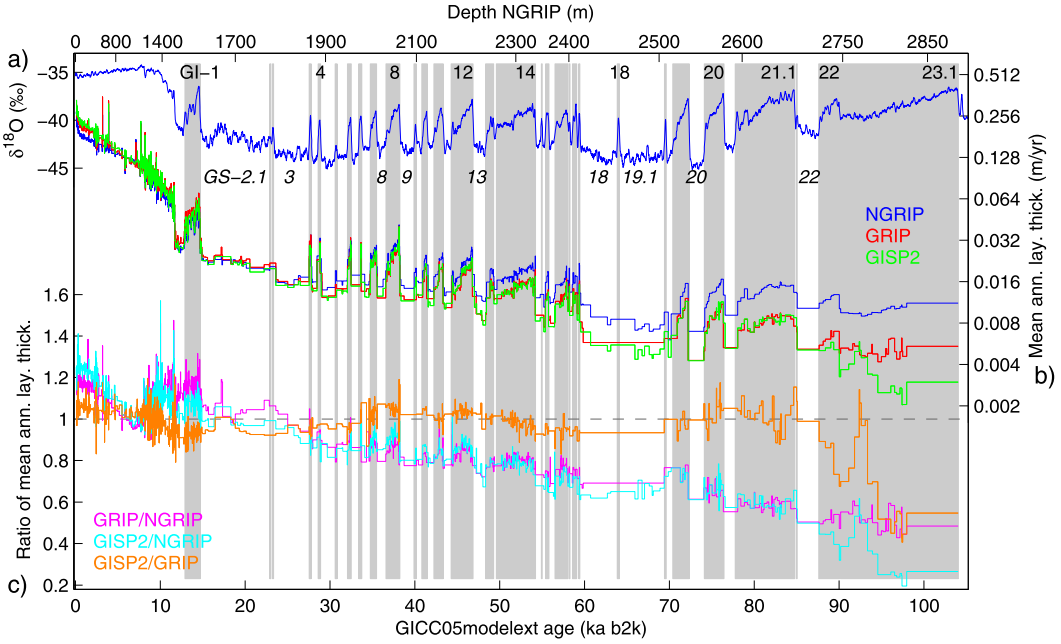

Fig. 7. Mean annual layer thicknesses (λ) and their respective ratios (r) on the GICC05modelext chronology. a) NGRIP δ^{18}O on the GICC05modelext timescale (bottom axis; corresponding NGRIP depths on top axis). Vertical grey bars represent interstadials, and selected GI numbers (black) and GS numbers (black italics) as defined by Rasmussen et al. (2014) are indicated. b) Mean annual layer thickness between neighbouring match points for each core (right logarithmic axis). c) Ratio of the annual layer thickness in one core to the other. The highly variable resolution of the λ and r curves with age is a reflection of the varying temporal density of match points (Section 2.1.4) and explains why some shorter interstadials are hardly visible in the λ profiles and that no variability of the layer thickness can be resolved across many stadials. Note that detailed layer thickness curves, are available also in sections without match points, but not shown here (see Section 2.3.2 and 3.2 for further explanation).

increase 19% higher than at NGRIP. As outlined in Section 3.1, large discrepancies between the GICC05 timescale and the GISP2 timescale may explain the very different accumulation rate responses calculated by Guillevic et al. (2013) for GRIP and GISP2 across the transition from GS-10 to GI-9. The observed stadial–interstadial contrast in the GRIP/NGRIP and GISP2/NGRIP r values suggests that the spatial accumulation gradient identified for GI-8 and GI-10 by Guillevic et al. (2013) may have been common to most D–O cycles. Between GRIP and GISP2 there is no consistent amplitude difference in λ across the D–O cycles.

3.2.2. *Relative layer thickness anomaly between the late glacial and early-to-mid-Holocene*

In addition to the variations between stadials and interstadials described above, interesting features that differ from the overall pattern are observed. This includes a pronounced change in relative layer thickness (r) between Summit and NGRIP in the late glacial and early-to-mid-Holocene. The section ~10–14.7 ka b2k is characterized by a relatively flat plateau of high GRIP/NGRIP ratios similar to modern values (around 1.2), whereas the mid-Holocene section is characterized by relatively low ratios reaching a local minimum of 0.95 at 6.9 ka (Fig. 7c). The GISP2/NGRIP ratios show the same overall pattern, but the contrast between the high values at the plateau and the low values at 6.9 ka b2k is smaller than for GRIP/NGRIP. The drop in GISP2/NGRIP and GRIP/NGRIP thickness ratios between ~10 ka b2k and 6.9 ka b2k coincides with significant thinning of the margins of the Greenland Ice Sheet and the Holocene climatic optimum (Vinther et al., 2009). The observed drop in relative layer thickness could be the result of altered flow conditions in response to the new ice-sheet geometry and/or changes in the accumulation pattern associated with the climatic optimum and the retreat of the margins. We speculate that the NGRIP site is more prone to changeable conditions due to its position relatively closer to the margin than the Summit sites.

3.2.3. *Variability between the two Summit sites*

GISP2 and GRIP layer thicknesses are typically within 10% of each other, except beyond ~87 ka b2k (see Section 2.4.2) and in a few short intervals where the fluctuations in layer thickness ratio can be ascribed to short-term accumulation variability or matchpoint uncertainty. Reconstructions of present day accumulation patterns show a zonal accumulation gradient in central Greenland, with higher accumulation rates on the western slope due to orographic uplift of westerly winds (Burgess et al., 2010). This gradient is reflected in a mean GISP2/GRIP layer thickness ratio of 1.06 over the last 300 years, as GISP2 is located 28 km to the west of the GRIP site. During the most recent ~9 ky, the GISP2 annual layer thickness typically exceeds the GRIP layer thickness, which suggests that the modern day east-west accumulation gradient in central Greenland has persisted through most of the Holocene. Looking at the long-term variations further back in time, we observe two periods where the GISP2 annual layers are generally thinner than those at GRIP: ~9–34 ka b2k and ~50–75 ka b2k (Figs. 7c and 2b). Possible explanations for these long-term variations in the GISP2/GRIP layer thickness ratio include altered flow conditions with possible ice divide migration (imprinted in the layer thickness profiles due to changed layer thinning) and/or changes in accumulation patterns. In the oldest part of the Summit cores we find strong changes in the layer thickness ratio presumably related to differential strain near the bed.

3.3. *Analysis of the parallel δ^{18}O climate records*

3.3.1. *Orbital and millennial-to-centennial-scale δ^{18}O gradients between the Summit (GRIP, GISP2) and NGRIP sites*

The GISP2, GRIP and NGRIP δ^{18}O records, now presented on one common chronology using our climate-independent synchronization method, display synchronous behaviour across GS/GI transitions at all sites within the precision of the synchronization and at

least within a 20-year resolution (Figs. 8a and 1 of Rasmussen et al. (2014)). Correlation coefficients between paired $\delta^{18}O$ profiles for the time interval 0–60 ka b2k range between 0.95 and 0.99 for 50-, 100- and 200-year averages, and between 0.85 and 0.90 for 5-, 10-, and 20-year averages. The highest correlation is obtained between GRIP and GISP2 $\delta^{18}O$ records irrespective of the time resolution, but the correlation coefficient is typically not more than 1 percentage point higher than for the two other core combinations. Although the $\delta^{18}O$ records agree on the timing of all large-amplitude centennial- and millennial-scale climate events, there is a slowly varying offset between the $\delta^{18}O$ levels in the NGRIP record and the two Summit cores (Fig. 8b) as also pointed out by North Greenland Ice Core Project Members (2004). The $\delta^{18}O$ level in the NGRIP record is 1–3‰ lower than in the Summit cores between GS-22 and the middle of GS-2.1, i.e. over most of the entire glacial period. The long-term (hereafter "orbital") variations in the $\delta^{18}O$ difference roughly follows changes in the North American Ice-Sheet volume (North Greenland Ice Core Project Members, 2004; Bintanja and van de Wal, 2008) with periods of large ice volume correlating with a large $\delta^{18}O$ gradient between central and northern Greenland. Our detailed chemo-stratigraphic synchronization reveals $\delta^{18}O$ differences on centennial and millennial timescales on top of the orbital $\delta^{18}O$-difference variations. The $\delta^{18}O$ contrast between the Summit cores and NGRIP is particularly large during the stadials in which Heinrich events are recorded in North Atlantic sediment cores. No systematic $\delta^{18}O$ difference is observed between the two Summit cores. A possible link between the periods of high millennial-to-centennial $\delta^{18}O$ gradients and Heinrich events will be discussed in Section 3.3.2, but first we discuss possible explanations of the observed changes in latitudinal $\delta^{18}O$ gradient.

3.3.1.1. Changes in regional temperature gradient in Greenland. Changes in the regional temperature field in Greenland towards relatively lower glacial temperatures at NGRIP compared to Summit could explain the glacial Summit–NGRIP $\delta^{18}O$ difference. However, results from model simulations of the Last Glacial Maximum (LGM) by Langen and Vinther (2009) point to a temperature gradient between Summit and NGRIP that is similar to that of modern conditions. Similarly on millennial timescales, the relative reduction of NGRIP $\delta^{18}O$ is observed mainly during stadials, and if caused by a stronger temperature gradient between Summit and NGRIP, this would require that NGRIP was anomalously cold or Summit anomalously warm during stadials. This is not supported by coupled climate simulations by Li et al. (2010) who on the contrary show that the temperature gradient is strongest during interstadials, because the Summit area is more sensitive than NGRIP to temperature increases over the ice-free Nordic Seas during the interstadials. Also, recent temperature reconstructions for NEEM, NGRIP and GISP2 for GI-8, GS-9, GI-10, GS-11 and the last deglaciation suggest that the northernmost sites experienced the smallest temperature contrast between stadial and interstadial conditions (Guillevic et al., 2013; Buizert et al., 2014). We thus consider it unlikely that the low stadial $\delta^{18}O$ values at NGRIP can be explained by a stronger temperature gradient between Summit and NGRIP compared to the present day.

3.3.1.2. Changes in mixing ratios of precipitation originating from different source regions with differential distillation histories due to different transport paths. The apparent relation between NAIS volume and the long-term variations in Summit–NGRIP $\delta^{18}O$ differences may be explained by the occurrence of a split jet stream around the North American Ice Sheet as demonstrated in model studies of LGM by Kutzbach and Guetter (1986) and Bromwich et al. (2004). The results suggest that the presence of NAIS is forcing the westerly upper-level flow to split into a southern branch traversing the southern modern USA and a northern branch flowing along the northern margin of the ice sheet, until the latter branch deflects southwards on the lee side of the NAIS to merge with the southern branch again. Along the northern branch, cyclones with a North Pacific origin can reach Greenland from the Northwest during the winter season when a pronounced split jet stream is active. The amount of precipitation coming from the Northwest is relatively low (<50 mm/year), but the effect can be significant because the $\delta^{18}O$ values of North Pacific moisture in Greenland are around 15‰ lower than for moisture coming from the North Atlantic (Charles et al., 1994). In line with Charles et al. (1995, 1994) who found a zonal pattern of air flow and moisture origin during the LGM with a sensitivity to glacial–interglacial temperature change of $0.8‰K^{-1}$ in North-Central Greenland compared to $0.4‰K^{-1}$ for Southeast Greenland, we find it likely that Northwest-sourced precipitation influenced the NGRIP site to a higher degree than the Summit sites.

The model simulation by Langen and Vinther (2009) suggests that sea surface temperatures (SSTs) and sea-ice extent play a more important role than topography (i.e. ice-sheet volume) for a shift from Atlantic to Pacific sources. The authors find that the contribution from the more distant and 'colder' Pacific source is happening during conditions with extensive sea-ice cover in the North Atlantic, and modest cooling of the tropics compared to present day conditions. Similar to Charles et al. (1994) they find that the Pacific contribution is largest in the north-western part of Greenland.

3.3.1.3. Changes in seasonality bias in the snowpack. Because of the large seasonal $\delta^{18}O$-amplitude in Greenland accumulation (~20‰) compared to the glacial-interglacial contrast (~8‰) (Steig et al., 1994), even a small change in the precipitation seasonality can lead to significant $\delta^{18}O$ differences. Several modelling studies suggest that compared to present-day conditions, Greenland winter precipitation was reduced during the cold glacial climate due to a southern displacement of the sea-ice edge in the Northern Atlantic, leading to a bias of mean-annual $\delta^{18}O$ towards less negative $\delta^{18}O$ values of summer precipitation (Krinner et al., 1997; Werner et al., 2000). The modelling experiment by Langen and Vinther (2009) shows that GRIP experienced a shift towards greater summer weighting compared to present-day due to extensive winter sea-ice cover in the North Atlantic. The northwestern part of Greenland, however, did not suffer much from this winter drying, resulting in a modelled NGRIP winter/summer accumulation ratio during the LGM close to the present-day value.

3.3.1.4. Changes in source-to-site distance and/or temperature gradient. The $\delta^{18}O$ differences can also be explained by a southward shift of the North Atlantic moisture source and the resulting change in the Rayleigh distillation process. The North Atlantic is believed to be the main moisture source for the NGRIP, GRIP and GISP2 sites at the present day (Charles et al., 1994; Werner et al., 2000, 2001; Langen and Vinther, 2009). A southward displacement of the North Atlantic moisture source due to ocean cooling and/or sea-ice expansion (e.g. Johnsen et al., 1989; Jouzel et al., 1995; Masson-Delmotte et al., 2005) leads to an increased distance and also a potentially larger temperature gradient between the source and the Greenland Ice Sheet. This increased source-to-site distance enhances the Rayleigh fractionation process resulting in lower $\delta^{18}O$ values in Greenland snow. A southward shift of the moisture source may also induce a $\delta^{18}O$ gradient between two sites located at different latitudes along the same distillation path because the non-linearity of a Rayleigh distillation process gets progressively larger toward the end of the moisture path. The location of NGRIP further away from the moisture source leads to relatively lower $\delta^{18}O$ values than at the Summit area.

3.3.1.5. Changes in elevation of the ice-sheet and upstream effects. Differences in elevation histories could account for some of the observed long-term $\delta^{18}O$ differences between Summit and NGRIP. An isotope difference of 3‰ would require that NGRIP experienced a relative elevation increase of 500 m compared to Summit, assuming an altitude effect of 0.6‰ per 100 m (Dansgaard, 1961; Johnsen et al., 1989). We find it likely that the ice bridge connecting the Greenland and the Innuitian Ice Sheets during periods of large ice volumes (England et al., 2006) may have changed the relative topography of the GIS, but we find relative elevation changes of several hundreds of metres unlikely in the interior of the ice sheet. A study of Holocene elevation changes showed that the relative difference in elevation changes between NGRIP and GRIP was only about 50 m during the breakdown of the bridge (Vinther et al., 2009), which is an order of magnitude less than what is needed to explain the 3‰ difference. Furthermore, elevation changes cannot explain the abrupt $\delta^{18}O$ differences anomalies on top of the slowly varying $\delta^{18}O$ difference.

3.3.1.6. Summary. We suggest that the observed Summit–NGRIP $\delta^{18}O$ differences during the Last Glacial can be explained by a relative increase of Pacific precipitation at NGRIP compared to at Summit, an increased summer bias in precipitation at Summit, and enhanced Rayleigh distillation due to an increased source-to-site distance leading to relatively more depleted $\delta^{18}O$ values at NGRIP. This happens in response to the presence of NAIS and the existence of a large sea-ice cover in the North Atlantic, both of which could cause the orbital-scale differences in $\delta^{18}O$ values seen between the Summit and the NGRIP records. Due to the relatively long dynamical response time of the large ice sheets, we believe that elevation changes of GIS, as well as NAIS-induced changes to the precipitation patterns in Greenland, are unlikely to have caused the observed $\delta^{18}O$ differences occurring on centennial-to-millennial timescales. Rapid changes in sea-ice cover and/or SST in the North Atlantic, however, seem to be a likely driving mechanism for these abrupt short-term $\delta^{18}O$-difference anomalies, especially in periods of ice rafting.

3.3.2. Possible Heinrich event imprint in Greenland ice cores

Among the most prominent glacial features in North Atlantic sediment cores are the so-called Heinrich Events, characterized by a high percentage of Ice Rafted Detritus (IRD) originating mainly (but not exclusively) from ice-berg discharge from the Laurentide Ice Sheet (Ruddiman, 1977; Heinrich, 1988; Bond et al., 1992; Broecker et al., 1992; Hemming, 2004). Until recently, no clear signature associated with the Heinrich events had been observed in the Greenland ice cores, but new data reveal that multiple ice-core proxies may record the atmospheric reorganization that accompanied Heinrich events (Severinghaus et al., 2009; Guillevic et al., 2014; Rhodes et al., 2014). Here we suggest that the Heinrich events are reflected in the latitudinal $\delta^{18}O$ gradient between ice-coring sites in Greenland.

The IRD layers are typically accompanied by low North Atlantic sea surface temperatures, low salinity and reduced North Atlantic Deep Water (NADW) formation (e.g. Keigwin and Lehman, 1994; Cortijo et al., 1997; Elliot et al., 2002; de Abreu et al., 2003). Climate proxies from middle to low latitudes around the globe suggest that a reorganization of the atmospheric circulation took place concomitant with the Heinrich events, and that the intertropical convergence zone (ITCZ) was shifted further south relative

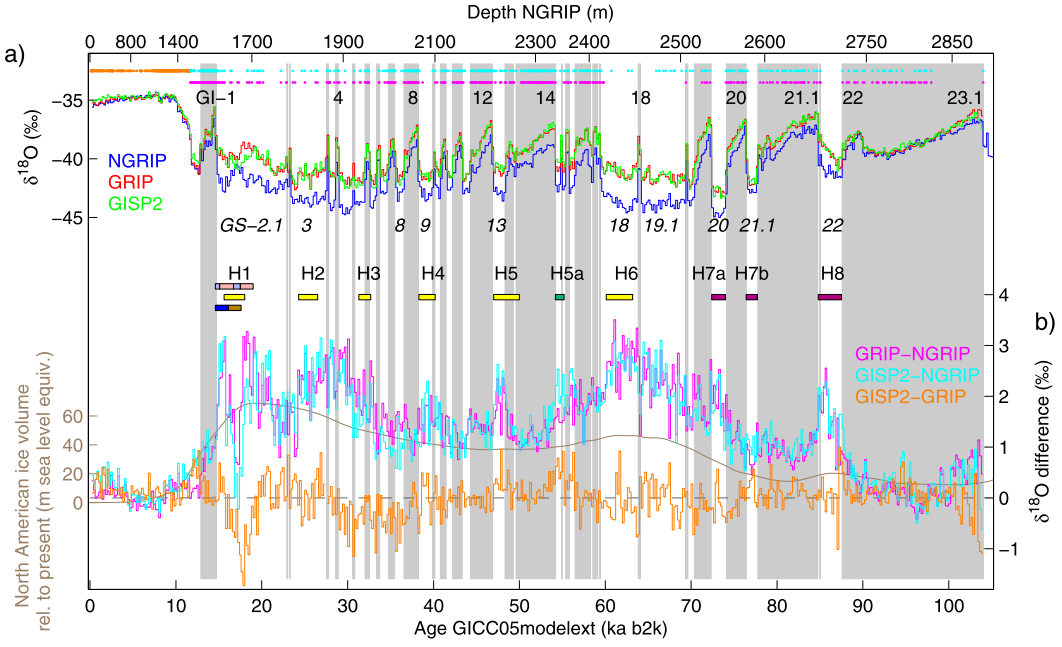

Fig. 8. Greenland water stable isotope profiles on the GICC05modelext timescale (bottom *x*-axis and corresponding NGRIP depths on top *x*-axis) and match points (dots on top) used for timescale transfer from NGRIP to GRIP (magenta) and GISP2 (cyan), respectively, and from GRIP to GISP2 (orange). a) $\delta^{18}O$ from the NGRIP (blue), GRIP (red) and GISP2 (green) ice cores in 200-year resolution. Vertical grey bars represent interstadial conditions, and black numbers above and below the $\delta^{18}O$ profiles indicate selected Greenland Interstadials (GI) and stadials (GS; in italics), as defined by Rasmussen et al. (2014). b) The difference in $\delta^{18}O$ value in one core relative to the other (right *y*-axis). On orbital timescales the GRIP–NGRIP (magenta) and GISP2–NGRIP (cyan) $\delta^{18}O$ difference look similar to the NAIS volume (light brown, left axis, presented on the original LR04 timescale). The timing and duration of the following events are shown in calendar ages: Heinrich (H) events 1,2,3,4,5 and 6 from Sanchez Goñi and Harrison (2010) (yellow boxes), four proposed substages of H1 from Stanford et al. (2011) (purple/light red boxes), and the two phases Big Dry and Big Wet (brown and blue) constituting the 'Mystery Interval' from Broecker and Putnam (2012). Timing of H5a, 7a, 7b and 8 is indicated relative to the D–O cycles in which they appear and are from Rashid et al. (2003) (bright blue) and Rasmussen et al. (2003) (purple). The naming and the ages of IRD events vary in the literature, especially for events older than H6 (e.g., Chapman and Shackleton, 1999; Hiscott et al., 2001; Ji et al., 2009). See text for a detailed discussion and $\delta^{18}O$ data references.

to normal stadial conditions (Boyle, 2000; Peterson et al., 2000; Wang et al., 2001; Clement et al., 2004; Chiang and Bitz, 2005; Chiang et al., 2008; Lewis et al., 2010; Cvijanovic and Chiang, 2013), most likely related to a greater sea-ice extent in the North Atlantic (Broecker, 2006). Indeed, SST reconstructions from e.g. marine core SU90-03 (at 40°N, 32°W) provide evidence that cold melt water intruded as far south as 40°N concurrent with Heinrich events (Chapman and Shackleton, 1998; Chapman et al., 2000). A greater sea-ice extent and lower North Atlantic sea surface temperatures (Cortijo et al., 2005; Eynaud et al., 2009) may be imprinted in Greenland as a greater Summit–NGRIP $\delta^{18}O$ difference than during a normal stadial, as outlined in Section 3.3.1.

Superimposed on the orbital-scale $\delta^{18}O$ difference in the glacial, Fig. 8b shows pronounced millennial-scale maxima of the Summit–NGRIP $\delta^{18}O$ difference, which seem to coincide with the occurrence of most of the Heinrich events between H8 and H1 (Rashid et al., 2003; Rasmussen et al., 2003; Sanchez Goñi and Harrison, 2010; Stanford et al., 2011). In the section corresponding to Marine Isotope Stage (MIS) 5 (older than 71 ka b2k; Lisiecki and Raymo (2005)), a pronounced positive anomaly is observed in the $\delta^{18}O$ difference curves during GS-22, a weaker anomaly in GS-20, while there is no observed anomaly in GS-21.1. Interestingly, the intrusion of iceberg laden polar waters reached further south during GS-22 and/or produced a stronger cooling than during the other Heinrich events observed during MIS 5 (McManus et al., 1994; Chapman and Shackleton, 1998, 1999; de Abreu et al., 2003; Martrat et al., 2007). This is in accordance with our interpretation that the largest $\delta^{18}O$ differences between Summit and NGRIP is reached during periods of large sea-ice cover (and/or low SSTs in the mid-Atlantic). During MIS 4 (71–57 ka) we observe gradually increasing $\delta^{18}O$ differences across most of GS-19.1 to GS-18 corresponding to a prolonged time interval of low and declining SST values observed in core SU90-03 at 40°N and also off the Iberian margin at the same latitude (Chapman and Shackleton, 1998; Chapman et al., 2000; de Abreu et al., 2003; Martrat et al., 2007). The maximum $\delta^{18}O$ difference towards the end of GS-18 seems coincident with the major ice rafting event H6. During the MIS 3 section (57–29 ka) there are positive anomalies in the Summit–NGRIP $\delta^{18}O$ difference corresponding to time intervals of SST minima related to H4 and H5, while an ice-core counterpart to H5a is seen in the GISP2–NGRIP difference curve only. It is hard to assign clear counterparts to H3 and H2 in the $\delta^{18}O$ difference curve, but we note that the declining $\delta^{18}O$ differences between ~30 ka and ~21 ka seem to appear during the same time interval (30–18 ka) as a gradual warming of SSTs in SU90-03, and that H2 and H3 seem to have had a minor impact on the SSTs in this area (Chapman and Shackleton, 1998; Chapman et al., 2000). The IRD deposition of H3 is even absent in core SU90-03, and is generally confined to more northerly latitudes and is geochemically distinct from H1, 2, 4 and 5 (Grousset et al., 1993; Hemming, 2004). Also, recent work by Lynch-Stieglitz et al. (2014) from the Florida Strait indicates that the Atlantic overturning circulation was not substantially reduced associated with H2 and H3, if reduced at all. Several studies (e.g. Eynaud et al., 2009) have suggested that the polar front did not reach as far south along the Iberian margin during the LGM as during Heinrich events, which could explain the relatively low $\delta^{18}O$ differences centred at GI-2.

Some of the most pronounced features in the $\delta^{18}O$ differences occur during the youngest part of the MIS 2 section (29–14 ka). In contrast to the general pattern during MIS 5–3, where stadials with Heinrich events seem to be associated with $\delta^{18}O$-difference maxima, we observe significant excursions between maximum and minimum values in the Summit–NGRIP $\delta^{18}O$ difference during the H1 rafting event, which may be related to different pulses of the H1 event (Bard et al., 2000; Stanford et al., 2011). Furthermore, the GRIP and GISP2 $\delta^{18}O$ values during the younger part of MIS 2 differ more than usual, as already discussed by Rasmussen et al. (2008). The observations suggest either that i) the H1 event is significantly different from the other Heinrich events, ii) the mechanisms to explain the relation between the Summit–NGRIP $\delta^{18}O$ difference and the H1 (and possibly H2 and H3) event are different from those related to the older Heinrich events, or iii) that the H1-signal in the $\delta^{18}O$ difference is overprinted by other processes related to the major reorganization of the atmospheric and oceanic circulation during the last termination (e.g. Steffensen et al., 2008; Denton et al., 2010; Okazaki et al., 2010). Indeed, climate proxies from around the world point to pronounced reorganization during the so-called Big Dry and Big Wet periods of the Mystery Interval, which is concurrent with the strong minimum in the Summit–NGRIP $\delta^{18}O$ difference and the following peak value, respectively (Denton et al., 2006; Broecker and Putnam, 2012) (Fig. 8b).

To conclude, while it seems that the Summit–NGRIP $\delta^{18}O$ difference shows anomalies during the stadials in which marine cores register H1, H4, H5, H5a, H7a and H8, it is more difficult to establish whether anomalies are also present in the remaining stadials that contain Heinrich events. Limitations in the relative dating precision and the resolution of the records make it impossible to determine to which degree the observed $\delta^{18}O$ differences are constrained to the periods of the Heinrich events themselves, or characterize a larger part of the stadials containing Heinrich events, but our study opens new paths for comparison of North Atlantic marine core SST proxies with Greenland ice-core records.

4. Summary and conclusions

The most recent chronology for Greenland ice cores, the GICC05modelext timescale, has been transferred to the entire undisturbed sections of the GRIP and GISP2 ice cores (0–104 ka b2k), based on a detailed chemo-stratigraphic matching method. We further provide GICC05modelext-consistent gas chronologies for both cores. Five tephra deposits, located in sections where no chemo-stratigraphic match points are observed, were also utilized for the timescale transfer, highlighting the value of cryptotephra isochrons for complementing the chemo-stratigraphic matching method (Rasmussen et al., 2013). Ongoing and future studies have the potential to reveal more tephra correlatives between the cores, enabling a further refinement of the synchronization.

A comparison with another widely used Greenland annual-layer-based chronology, the GISP2 timescale, shows that the GISP2 timescale implies an inconsistent relationship between $\delta^{18}O$ and annual layer thickness across D–O cycles. Consequently, the duration estimates for individual GSs and GIs differ substantially from those obtained from GICC05 (Fig. 6). On average, the stadial duration obtained from the GISP2 timescale is 15% shorter and the interstadial duration 15% longer compared to the duration estimates derived from GICC05, implying that the choice of timescale has major influence on the interpretation of past climatic events in Greenland.

Based on the depth–depth relationship from the matching, we conclude that the Summit region on average experienced an ~10% higher accumulation increase compared to NGRIP going from stadial to interstadial conditions during the Last Glacial, and we observe a pronounced change in the ratio of layer thickness r between Summit and NGRIP across the Last Glacial termination and early-to-mid Holocene (Fig. 7). Our results show the necessity for future ice flow models to incorporate the observed depth–depth relationships to account for and distinguish between changes in e.g. flow pattern, ice-sheet geometry and relative accumulation changes.

The NGRIP, GRIP and GISP2 $\delta^{18}O$ records on the common GICC05modelext timescale show synchronous behaviour at the abrupt shifts between GSs and GIs (Fig. 8). Overall similar climatic

conditions over the Last Glacial-Interglacial cycle are indicated by high correlation coefficients between the $\delta^{18}O$ temperature-proxy records. However, the Summit–NGRIP $\delta^{18}O$ difference reveals offsets during the Last Glacial that we believe are caused by a relative increase of precipitation of Pacific origin at NGRIP, a shift towards a stronger summer weighting of snow fall at Summit, and an enhanced Rayleigh fractionation, leading to relatively lower $\delta^{18}O$ values at NGRIP. We suggest that the orbital-scale $\delta^{18}O$ differences may be induced by the general glacial boundary conditions, i.e. the presence of the North American Ice Sheet, reduced temperatures and larger sea-ice extent. Likely mechanisms to explain the millennial-to-centennial-scale anomalies observed in the Summit–NGRIP $\delta^{18}O$ difference are changing sea-ice extent and/or SSTs in the North Atlantic linked to major ice rafting events. Except for Heinrich events H2 and H3 during MIS 2, we find that anomalies in the Summit–NGRIP $\delta^{18}O$ difference are observed during stadials containing Heinrich events, probably associated with southwards expansion of polar water and possibly latitudinal migration of the polar front. During the youngest part of MIS 2 and the deglaciation, the interpretation is more complex, but the $\delta^{18}O$ difference seems to register phases that may be related to the Big Dry and Big Wet of the Mystery Interval. Future isotope modelling should help decipher to what extent the proposed mechanisms can explain the temporal changes in latitudinal $\delta^{18}O$ gradients, and we hope that this assertion of an ice-core $\delta^{18}O$ imprint of Heinrich events will motivate further studies of the interplay between stadial climate and Heinrich events. The realization that Heinrich events seem to be reflected in the Greenland ice-core record through the impact of ice rafting on North Atlantic sea-ice extent and atmospheric reorganization could motivate the development of new proxies, e.g. impurity records for constraining North Atlantic sea-ice extent.

With this work and the recent work of Rasmussen et al. (2013) the four Greenland deep ice cores NEEM, NGRIP, GRIP and GISP2 are now tied to the same chronology, GICC05modelext, for the full length of their undisturbed sections of both the ice and gas phases. It is our hope that the continued efforts to provide a consistent chronological framework for multiple cores will facilitate and inspire new studies into the inter-core differences and provide a deeper understanding of the governing mechanisms of glacial as well as interglacial climatic change.

Acknowledgements

This study is a contribution to the INTIMATE project, supported by INQUA (INQUA Focus Group & project 1210F) and funded as the EU COST Action ES0907, and to the RESOLuTION project, part of the EuroCLIMATE ESF-EUROCORES programme, supported by The Danish Council for Independent Research, Natural Sciences (FNU). PMA, AJB, EC and SMD have received funding from the European Research Council under the European Union's Seventh Framework Programme (FP7/2007–2013)/TRACE project: ERC grant agreement no. [259253]. PMA, AJB, EC and SMD acknowledge the support of the Climate Change Consortium of Wales (C3W). The new GISP2 $\delta^{15}N$ measurements were supported by NSF grants 97–25305 and 99–05241 (to JPS). We thank Anette Mortensen and Karl Grönvold for assistance with the tephra work, Antje Voelker and Jesper Olsen for fruitful discussions on Heinrich events and the Summit-NGRIP $\delta^{18}O$-difference signal, and two anonymous reviewers for constructive and helpful comments, which improved the manuscript significantly. Thanks also to the many individuals and organizations involved in NGRIP, GRIP, and GISP2 logistics, drill development, drilling, as well as ice-core processing and analysis. NGRIP is directed and organized by the Ice and Climate Research Group, Niels Bohr Institute, University of Copenhagen. It was supported by funding agencies in Denmark (Forskningsrådet for Natur og Univers), Belgium (Fonds National de la Recherche Scientifique), France (Institut Polaire Français and Institut National des Science de l'Univers/CNRS), Germany (AWI), Iceland (Rannís), Japan (Ministry of Education, Culture, Sports, Science and Technology), Sweden (Polarforskningssekretariatet), Switzerland (Der Schweizerische Nationalfonds) and the United States (NSF, Office of Polar Programs).

Appendix A. Supplementary data

Supplementary data related to this article can be found at http://dx.doi.org/10.1016/j.quascirev.2014.10.032. Data files are also available from http://www.iceandclimate.nbi.ku.dk/data.

References

Abbott, P.M., Davies, S.M., Steffensen, J.P., Pearce, N.J.G., Bigler, M., Johnsen, S.J., Seierstad, I.K., Svensson, A., Wastegård, S., 2012. A detailed framework of Marine Isotope Stages 4 and 5 volcanic events recorded in two Greenland ice-cores. Quat. Sci. Rev. 36, 59–77.

Alley, R.B., Meese, D.A., Shuman, C.A., Gow, A.J., Taylor, K.C., Grootes, P.M., White, J.W.C., Ram, M., Waddington, E.D., Mayewski, P.A., Zielinski, G.A., 1993. Abrupt increase in Greenland snow accumulation at the end of the Younger Dryas event. Nature 362, 527–529.

Alley, R.B., Shuman, C.A., Meese, D.A., Gow, A.J., Taylor, K.C., Cuffey, K.M., Fitzpatrick, J.J., Grootes, P.M., Zielinski, G.A., Ram, M., Spinelli, G., Elder, B., 1997. Visual-stratigraphic dating of the GISP2 ice core: basis, reproducibility, and application. J. Geophys. Res. 102, 26367–26382.

Andersen, K.K., Svensson, A., Rasmussen, S.O., Steffensen, J.P., Johnsen, S.J., Bigler, M., Röthlisberger, R., Ruth, U., Siggaard-Andersen, M.-L., Dahl-Jensen, D., Vinther, B.M., Clausen, H.B., 2006. The Greenland ice core chronology 2005, 15–42 ka. Part 1: constructing the time scale. Quat. Sci. Rev. 25, 3246–3257.

Bard, E., Rostek, F., Turon, J.-L., Gendreau, S., 2000. Hydrological impact of Heinrich event in the subtropical Northeast Atlantic. Science 289, 1321–1324.

Bender, M., Sowers, T., Dickson, M.-L., Orchardo, J., Grootes, P., Mayewski, P.A., Meese, D.A., 1994. Climate correlations between Greenland and Antarctica during the past 100,000 years. Nature 372, 663–666.

Bigler, M., 2004. Hochauflösende Spurenstoffmessungen an polaren Eisbohrkernen: Glazio-chemische und klimatische Prozessstudien. Physics Institute. University of Bern, Switzerland.

Bintanja, R., van de Wal, R.S.W., 2008. North American ice-sheet dynamics and the onset of 100,000-year glacial cycles. Nature 454, 869–872.

Blockley, S.P.E., Lane, C.S., Hardiman, M., Rasmussen, S.O., Seierstad, I.K., Steffensen, J.P., Svensson, A., Lotter, A.F., Turney, C.S.M., Bronk Ramsey, C., 2012. Synchronisation of palaeoenvironmental records over the last 60,000 years, and an extended INTIMATE event stratigraphy to 48,000 b2k. Quat. Sci. Rev. 36, 2–10.

Blunier, T., Brook, E.J., 2001. Timing of millennial-scale climate change in Antarctica and Greenland during the Last Glacial period. Science 291, 109–112.

Bond, G., Heinrich, H., Broecker, W., Labeyrie, L., McManus, J., Andrews, J., Huon, S., Jantschik, R., Clasen, S., Simet, C., Tedesco, K., Klas, M., Bonani, G., Ivy, S., 1992. Evidence for massive discharges of icebergs into the North Atlantic Ocean during the Last Glacial period. Nature 360, 245–249.

Bourne, A.J., Cook, E., Abbott, P.M., Seierstad, I.K., Steffensen, J.P., Svensson, A., Schüpbach, S., Fischer, H., Davies, S.M., 2014. A tephra lattice for Greenland and a reconstruction of volcanic events spanning 25–45 ka b2k. Quat. Sci. Rev. http://dx.doi.org/10.1016/j.quascirev.2014.07.017.

Bourne, A.J., Davies, S.M., Abbott, P.M., Rasmussen, S.O., Steffensen, J.P., Svensson, A., 2013. Revisiting the Faroe Marine Ash Zone III in two Greenland ice cores: implications for marine-ice correlations. J. Quat. Sci. 28, 641–646.

Boyle, E.A., 2000. Is ocean thermohaline circulation linked to abrupt stadial/interstadial transitions? Quat. Sci. Rev. 19, 255–272.

Broecker, W., Bond, G., Klas, M., Clark, E., McManus, J., 1992. Origin of the Northern Atlantic's Heinrich events. Clim. Dyn. 6, 265–273.

Broecker, W., Putnam, A.E., 2012. How did the hydrologic cycle respond to the two-phase mystery interval? Quat. Sci. Rev. 57, 17–25.

Broecker, W.S., 2006. Abrupt climate change revisited. Glob. Planet. Change 54, 211–215.

Bromwich, D.H., Toracinta, E.R., Wei, H., Oglesby, R.J., Fastook, J.L., Hughes, T.J., 2004. Polar MM5 simulations of the winter climate of the Laurentide Ice Sheet at the LGM. J. Clim. 17, 3415–3433.

Brook, E.J., Harder, S., Severinghaus, J., Steig, E.J., Sucher, C.M., 2000. On the origin and timing of rapid changes in atmospheric methane during the Last Glacial period. Glob. Biogeochem. Cycles 14, 559–572.

Brook, E.J., Severinghaus, J.P., 2011. Methane and megafauna. Nat. Geosci. 4, 271–272.

Brook, E.J., Sowers, T., Orchardo, J., 1996. Rapid variations in atmospheric methane concentration during the past 110,000 years. Science 273, 1087–1091.

Buizert, C., Gkinis, V., Severinghaus, J.P., He, F., Lecavalier, B.S., Kindler, P., Leuenberger, M., Carlson, A.E., Vinther, B., Masson-Delmotte, V., White, J.W.C., Liu, Z., Otto-Bliesner, B., Brook, E.J., 2014. Greenland temperature response to climate forcing during the last deglaciation. Science 345, 1177–1180.

Buizert, C., Martinerie, P., Petrenko, V.V., Severinghaus, J.P., Trudinger, C.M., Witrant, E., Rosen, J.L., Orsi, A.J., Rubino, M., Etheridge, D.M., Steele, L.P., Hogan, C., Laube, J.C., Sturges, W.T., Levchenko, V.A., Smith, A.M., Levin, I., Conway, T.J., Dlugokencky, E.J., Lang, P.M., Kawamura, K., Jenk, T.M., White, J.W.C., Sowers, T., Schwander, J., Blunier, T., 2012. Gas transport in firn: multiple-tracer characterisation and model intercomparison for NEEM, Northern Greenland. Atmos. Chem. Phys. 12, 4259–4277.

Buizert, C., Sowers, T., Blunier, T., 2013. Assessment of diffusive isotopic fractionation in polar firn, and application to ice core trace gas records. Earth Planet. Sci. Lett. 361, 110–119.

Burgess, E.W., Forster, R.R., Box, J.E., Mosley-Thompson, E., Bromwich, D.H., Bales, R.C., Smith, L.C., 2010. A spatially calibrated model of annual accumulation rate on the Greenland Ice Sheet (1958–2007). J. Geophys. Res. Earth Surf. 115, F02004.

Chapman, M.R., Shackleton, N.J., 1998. Millennial-scale fluctuations in North Atlantic heat flux during the last 150,000 years. Earth Planet. Sci. Lett. 159, 57–70.

Chapman, M.R., Shackleton, N.J., 1999. Global ice-volume fluctuations, North Atlantic ice-rafting events, and deep-ocean circulation changes between 130 and 70 ka. Geology 27, 795–798.

Chapman, M.R., Shackleton, N.J., Duplessy, J.-C., 2000. Sea surface temperature variability during the Last Glacial–Interglacial cycle: assessing the magnitude and pattern of climate change in the North Atlantic. Palaeogeogr. Palaeoclimatol. Palaeoecol. 157, 1–25.

Charles, C.D., Rind, D., Jouzel, J., Koster, R.D., Fairbanks, R.G., 1994. Glacial–interglacial changes in moisture sources for Greenland: Influences on the ice core record of climate. Science 263, 508–511.

Charles, C.D., Rind, D., Jouzel, J., Koster, R.D., Fairbanks, R.G., 1995. Seasonal precipitation timing and ice core records. Science 269, 247–248.

Chiang, J.C.H., Bitz, C.M., 2005. Influence of high latitude ice cover on the marine Intertropical Convergence Zone. Clim. Dyn. 25, 477–496.

Chiang, J.C.H., Cheng, W., Bitz, C.M., 2008. Fast teleconnections to the tropical Atlantic sector from Atlantic thermohaline adjustment. Geophys. Res. Lett. 35, L07704.

Clausen, H.B., Hammer, C.U., Hvidberg, C.S., Dahl-Jensen, D., Steffensen, J.P., Kipfstuhl, J., Legrand, M., 1997. A comparison of the volcanic records over the past 4000 years from the Greenland Ice Core Project and Dye 3 Greenland ice cores. J. Geophys. Res. 102, 26707–26723.

Clement, A.C., Hall, A., Broccoli, A.J., 2004. The importance of precessional signals in the tropical climate. Clim. Dyn. 22, 327–341.

Cortijo, E., Duplessy, J.-C., Labeyrie, L., Duprat, J., Paillard, D., 2005. Heinrich events: hydrological impact. C. R. Geosci. 337, 897–907.

Cortijo, E., Labeyrie, L., Vidal, L., Vautravers, M., Chapman, M., Duplessy, J.-C., Elliot, M., Arnold, M., Turon, J.-L., Auffret, G., 1997. Changes in sea surface hydrology associated with Heinrich event 4 in the North Atlantic Ocean between 40° and 60°N. Earth Planet. Sci. Lett. 146, 29–45.

Coulter, S.E., Pilcher, J.R., Plunkett, G., Baillie, M., Hall, V.A., Steffensen, J.P., Vinther, B.M., Clausen, H.B., Johnsen, S.J., 2012. Holocene tephras highlight complexity of volcanic signals in Greenland ice cores. J. Geophys. Res. Atmos. 117, D21303.

Cuffey, K.M., Clow, G.D., 1997. Temperature, accumulation, and ice sheet elevation in central Greenland through the last deglacial transition. J. Geophys. Res. 102, 26383–26396.

Cuffey, K.M., Paterson, W.S.B., 2010. The Physics of Glaciers, fourth ed. Butterworth-Heinemann, Oxford, UK.

Cvijanovic, I., Chiang, J.H., 2013. Global energy budget changes to high latitude North Atlantic cooling and the tropical ITCZ response. Clim. Dyn. 40, 1435–1452.

Dahl-Jensen, D., Gundestrup, N., Miller, H., Watanabe, O., Johnsen, S.J., Steffensen, J.P., Clausen, H.B., Svensson, A., Larsen, L.B., 2002. The NorthGRIP deep drilling program. Ann. Glaciol. 35, 1–4.

Dansgaard, W., 1961. The isotopic composition of natural waters. Medd. Grønl. 165, 120.

Davies, S.M., Abbott, P.M., Meara, R.H., Pearce, N.J.G., Austin, W.E.N., Chapman, M.R., Svensson, A., Bigler, M., Rasmussen, T.L., Rasmussen, S.O., Farmer, E.J., 2014. A North Atlantic tephrostratigraphical framework for 130–60 ka b2k: new tephra discoveries, marine-based correlations, and future challenges. Quat. Sci. Rev. 106, 101–121.

Davies, S.M., Wastegaard, S., Abbott, P.M., Barbante, C., Bigler, M., Johnsen, S.J., Rasmussen, T.L., Steffensen, J.P., Svensson, A., 2010. Tracing volcanic events in the NGRIP ice-core and synchronising North Atlantic marine records during the Last Glacial period. Earth Planet. Sci. Lett. 294.

de Abreu, L., Shackleton, N.J., Schönfeld, J., Hall, M., Chapman, M., 2003. Millennial-scale oceanic climate variability off the Western Iberian margin during the last two glacial periods. Mar. Geol. 196, 1–20.

Denton, G.H., Anderson, R.F., Toggweiler, J.R., Edwards, R.L., Schaefer, J.M., Putnam, A.E., 2010. The Last Glacial termination. Science 328, 1652–1656.

Denton, G.H., Broecker, W.S., Alley, R.B., 2006. The mystery interval 17.5 to 14.5 kyrs ago. Pages News 14, 14–16.

Elliot, M., Labeyrie, L., Duplessy, J.-C., 2002. Changes in North Atlantic deep-water formation associated with the Dansgaard–Oeschger temperature oscillations (60–10 ka). Quat. Sci. Rev. 21, 1153–1165.

Elsässer, C., Wagenbach, D., Levin, I., Stanzick, A., Christl, M., Wallner, A., Kipfstuhl, S., Seierstad, I.K., Wershofen, H., Dibb, J., 2014. Simulating ice core ^{10}Be on the glacial–interglacial timescale. Clim. Past Discuss. 10, 761–808.

England, J., Atkinson, N., Bednarski, J., Dyke, A.S., Hodgson, D.A., Ó Cofaigh, C., 2006. The Innuitian Ice Sheet: configuration, dynamics and chronology. Quat. Sci. Rev. 25, 689–703.

Eynaud, F., de Abreu, L., Voelker, A., Schönfeld, J., Salgueiro, E., Turon, J.-L., Penaud, A., Toucanne, S., Naughton, F., Sánchez Goñi, M.F., Malaizé, B., Cacho, I., 2009. Position of the Polar Front along the western Iberian margin during key cold episodes of the last 45 ka. Geochem. Geophys. Geosyst. 10, Q07U05.

Flückiger, J., Blunier, T., Stauffer, B., Chappellaz, J., Spahni, R., Kawamura, K., Schwander, J., Stocker, T.F., Dahl-Jensen, D., 2004. N_2O and CH_4 variations during the Last Glacial epoch: insight into global processes. Glob. Biogeochem. Cycles 18, GB1020. http://dx.doi.org/10.1029/2003GB002122.

Freitag, J., Kipfstuhl, S., Laepple, T., Wilhelms, F., 2013. Impurity-controlled densification: a new model for stratified polar firn. J. Glaciol. 59, 1163–1169.

Fuhrer, K., Neftel, A., Anklin, M., Maggi, V., 1993. Continuous measurements of hydrogen peroxide, formaldehyde, calcium and ammonium concentrations along the new GRIP ice core from Summit, Central Greenland. Atmos. Environ. A27, 1873–1880.

Fuhrer, K., Neftel, A., Anklin, M., Staffelbach, T., Legrand, M., 1996. High-resolution ammonium ice core record covering a complete glacial-interglacial cycle. J. Geophys. Res. Atmos. 101, 4147–4164.

Goujon, C., Barnola, J.-M., Ritz, C., 2003. Modeling the densification of polar firn including heat diffusion: application to close-off characteristics and gas isotopic fractionation for Antarctica and Greenland sites. J. Geophys. Res. 108, 4792. http://dx.doi.org/10.1029/2002JD003319.

Gow, A.J., Meese, D.A., Alley, R.B., Fitzpatrick, J.J., Anandakrishnan, S., Woods, G.A., Elder, B.C., 1997. Physical and structural properties of the Greenland Ice Sheet Project 2 ice core: a review. J. Geophys. Res. 102, 26559–26575.

Grachev, A.M., Brook, E.J., Severinghaus, J.P., 2007. Abrupt changes in atmospheric methane at the MIS 5b–5a transition. Geophys. Res. Lett. 34, L20703.

Grönvold, K., Óskarsson, N., Johnsen, S.J., Clausen, H.B., Hammer, C.U., Bond, G., Bard, E., 1995. Ash layers from Iceland in the Greenland GRIP ice core correlated with oceanic and land sediments. Earth Planet. Sci. Lett. 135, 149–155.

Grootes, P.M., Stuiver, M., 1997. Oxygen 18/16 variability in Greenland snow and ice with 10^{-3}- to 10^{5}-year time resolution. J. Geophys. Res. 102, 26455–26470.

Grootes, P.M., Stuiver, M., White, J.W.C., Johnsen, S.J., Jouzel, J., 1993. Comparison of oxygen isotope records from the GISP2 and GRIP Greenland ice cores. Nature 366, 552–554.

Grousset, F.E., Labeyrie, L., Sinko, J.A., Cremer, M., Bond, G., Duprat, J., Cortijo, E., Huon, S., 1993. Patterns of ice-rafted detritus in the glacial North Atlantic (40–55°N). Paleoceanography 8, 175–192.

Guillevic, M., Bazin, L., Landais, A., Kindler, P., Orsi, A., Masson-Delmotte, V., Blunier, T., Buchardt, S.L., Capron, E., Leuenberger, M., Martinerie, P., Prié, F., Vinther, B.M., 2013. Spatial gradients of temperature, accumulation and δ^{18}O-ice in Greenland over a series of Dansgaard-Oeschger events. Clim. Past 9, 1029–1051.

Guillevic, M., Bazin, L., Landais, A., Stowasser, C., Masson-Delmotte, V., Blunier, T., Eynaud, F., Falourd, S., Michel, E., Minster, B., Popp, T., Prié, F., Vinther, B.M., 2014. Evidence for a 3 phase sequence during Heinrich Stadial 4 using a multiproxy approach based on Greenland ice core records. Clim. Past. Accepted for publication.

Heinrich, H., 1988. Origin and consequences of cyclic ice rafting in the northeast Atlantic Ocean during the past 130,000 years. Quat. Res. 29, 142–152.

Hemming, S.R., 2004. Heinrich events: massive late Pleistocene detritus layers of the North Atlantic and their global climate imprint. Rev. Geophys. 42, RG1005. http://dx.doi.org/10.1029/2003RG000128.

Herron, M.M., Langway Jr., C.C., 1980. Firn densification: an empirical model. J. Glaciol. 25, 373–385.

Hiscott, R.N., Aksu, A.E., Mudie, P.J., Parsons, D.F., 2001. A 340,000 year record of ice rafting, palaeoclimatic fluctuations, and shelf-crossing glacial advances in the southwestern Labrador Sea. Glob. Planet. Change 28, 227–240.

Huber, C., Leuenberger, M., Spahni, R., Flückiger, J., Schwander, J., Stocker, T.F., Johnsen, S., Landais, A., Jouzel, J., 2006. Isotope calibrated Greenland temperature record over Marine Isotope Stage 3 and its relation to CH_4. Earth Planet. Sci. Lett. 243, 504–519.

Huybers, P., Langmuir, C., 2009. Feedback between deglaciation, volcanism, and atmospheric CO_2. Earth Planet. Sci. Lett. 286, 479–491.

Ji, J., Ge, Y., Balsam, W., Damuth, J.E., Chen, J., 2009. Rapid identification of dolomite using a Fourier Transform Infrared Spectrophotometer (FTIR): a fast method for identifying Heinrich events in IODP Site U1308. Mar. Geol. 258, 60–68.

Johnsen, S.J., Clausen, H.B., Dansgaard, W., Fuhrer, K., Gundestrup, N., Hammer, C.U., Iversen, P., Steffensen, J.P., Jouzel, J., Stauffer, B., 1992. Irregular glacial interstadials recorded in a new Greenland ice core. Nature 359, 311–313.

Johnsen, S.J., Clausen, H.B., Dansgaard, W., Gundestrup, N.S., Hammer, C.U., Andersen, U., Andersen, K.K., Hvidberg, C.S., Dahl-Jensen, D., Steffensen, J.P., Shoji, H., Sveinbjörnsdóttir, Á.E., White, J., Jouzel, J., Fisher, D., 1997. The δ^{18}O record along the Greenland Ice Core Project deep ice core and the problem of possible Eemian climatic instability. J. Geophys. Res. 102, 26397–26410.

Johnsen, S.J., DahlJensen, D., Gundestrup, N., Steffensen, J.P., Clausen, H.B., Miller, H., Masson-Delmotte, V., Sveinbjornsdottir, A.E., White, J., 2001. Oxygen isotope and palaeotemperature records from six Greenland ice-core stations: Camp Century, Dye-3, GRIP, GISP2, Renland and NorthGRIP. J. Quat. Sci. 16, 299–307.

Johnsen, S.J., Dansgaard, W., White, J.W.C., 1989. The origin of Arctic precipitation under present and glacial conditions. Tellus B 41, 452–468.
Jouzel, J., Vaikmae, R., Petit, J.R., Martin, M., Duclos, Y., Stievenard, M., Lorius, C., Toots, M., Mélières, M.A., Burckle, L.H., Barkov, N.I., Kotlyakov, V.M., 1995. The two-step shape and timing of the last deglaciation in Antarctica. Clim. Dyn. 11, 151–161.
Jouzel, J., Vimeux, F., Caillon, N., Delaygue, G., Hoffmann, G., Masson-Delmotte, V., Parrenin, F., 2003. Magnitude of isotope/temperature scaling for interpretation of central Antarctic ice cores. J. Geophys. Res. 108, 4361. http://dx.doi.org/10.1029/2002JD002677.
Karlsson, N.B., Dahl-Jensen, D., Gogineni, S.P., Paden, J.D., 2013. Tracing the depth of the Holocene ice in North Greenland from radio-echo sounding data. Ann. Glaciol. 54, 44–50.
Keigwin, L.D., Lehman, S.J., 1994. Deep circulation change linked to Heinrich event 1 and Younger Dryas in a middepth North Atlantic core. Paleoceanography 9, 185–194.
Kindler, P., Guillevic, M., Baumgartner, M., Schwander, J., Landais, A., Leuenberger, M., 2014. Temperature reconstruction from 10 to 120 kyr b2k from the NGRIP ice core. Clim. Past 10, 887–902.
Kobashi, T., Severinghaus, J.P., Barnola, J.M., 2008a. 4 +/− 1.5 degrees C abrupt warming 11,270 yr ago identified from trapped air in Greenland ice. Earth Planet. Sci. Lett. 268, 397–407.
Kobashi, T., Severinghaus, J.P., Brook, E.J., Barnola, J.M., Grachev, A.M., 2007. Precise timing and characterization of abrupt climate change 8200 years ago from air trapped in polar ice. Quat. Sci. Rev. 26, 1212–1222.
Kobashi, T., Severinghaus, J.P., Kawamura, K., 2008b. Argon and nitrogen isotopes of trapped air in the GISP2 ice core during the Holocene epoch (0–11,500 B.P.): methodology and implications for gas loss processes. Geochim. Cosmochim. Acta 72, 4675–4686.
Krinner, G., Genthon, C., Jouzel, J., 1997. GCM analysis of local influences on ice core δ signals. Geophys. Res. Lett. 24, 2825–2828.
Kutzbach, J.E., Guetter, P.J., 1986. The influence of changing orbital parameters and surface boundary conditions on climate simulations for the past 18,000 years. J. Atmos. Sci. 43, 1726–1759.
Landais, A., Caillon, N., Goujon, C., Grachev, A.M., Barnola, J.M., Chappellaz, J., Jouzel, J., Masson-Delmotte, V., Leuenberger, M., 2004. Quantification of rapid temperature change during DO event 12 and phasing with methane inferred from air isotopic measurements. Earth Planet. Sci. Lett. 225, 221–232.
Landais, A., Chappellaz, J., Delmotte, M., Jouzel, J., Blunier, T., Bourg, C., Caillon, N., Cherrier, S., Malaize, B., Masson-Delmotte, V., Raynaud, D., Schwander, J., Steffensen, J.P., 2003. A tentative reconstruction of the Last Interglacial and Glacial inception in Greenland based on new gas measurements in the Greenland Ice Core Project (GRIP) ice core. J. Geophys. Res. Atmos. 108.
Lang, C., Leuenberger, M., Schwander, J., Johnsen, S., 1999. 16 °C rapid temperature variation in Central Greenland 70,000 years ago. Science 286, 934–937.
Langen, P.L., Vinther, B.M., 2009. Response in atmospheric circulation and sources of Greenland precipitation to glacial boundary conditions. Clim. Dyn. 32, 1035–1054.
Leuenberger, M., Lang, C., Schwander, J., 1999. Delta ^{15}N measurements as a calibration tool for the paleothermometer and gas-ice age differences: a case study for the 8200 B.P. event on GRIP ice. J. Geophys. Res. 104, 22163–22170.
Lewis, S.C., LeGrande, A.N., Kelley, M., Schmidt, G.A., 2010. Water vapour source impacts on oxygen isotope variability in tropical precipitation during Heinrich events. Clim. Past 6, 325–343.
Li, C., Battisti, D.S., Bitz, C.M., 2010. Can North Atlantic Sea Ice Anomalies account for Dansgaard–Oeschger climate signals? J. Clim. 23, 5457–5475.
Lisiecki, L.E., Raymo, M.E., 2005. A Pliocene–Pleistocene stack of 57 globally distributed benthic $\delta^{18}O$ records. Paleoceanography 20, PA1003.
Lynch-Stieglitz, J., Schmidt, M.W., Gene Henry, L., Curry, W.B., Skinner, L.C., Mulitza, S., Zhang, R., Chang, P., 2014. Muted change in Atlantic overturning circulation over some glacial-aged Heinrich events. Nat. Geosci. 7, 144–150.
Martinerie, P., Lipenkov, V.Y., Raynaud, D., Chappellaz, J., Barkov, N.I., Lorius, C., 1994. Air content paleo record in the Vostok ice core (Antarctica): a mixed record of climatic and glaciological parameters. J. Geophys. Res. 99, 10565–10576.
Martrat, B., Grimalt, J.O., Shackleton, N.J., de Abreu, L., Hutterli, M.A., Stocker, T.F., 2007. Four climate cycles of recurring deep and surface water destabilizations on the Iberian margin. Science 317, 502–507.
Masson-Delmotte, V., Jouzel, J., Landais, A., Stievenard, M., Johnsen, S.J., White, J.W.C., Werner, M., Sveinbjornsdottir, A., Fuhrer, K., 2005. GRIP deuterium excess reveals rapid and orbital-scale changes in Greenland moisture origin. Science 309, 118–121.
Mayewski, P.A., Meeker, L.D., Twickler, M.S., Whitlow, S., Yang, Q.Z., Lyons, W.B., Prentice, M., 1997. Major features and forcing of high-latitude northern hemisphere atmospheric circulation using a 110,000-year-long glaciochemical series. J. Geophys. Res. Oceans 102, 26345–26366.
McManus, J.F., Bond, G.C., Broecker, W.S., Johnsen, S.J., Labeyrie, L., Higgins, S., 1994. High-resolution climate records from the North Atlantic during the Last Interglacial. Nature 371, 326–329.
Meese, D.A., Gow, A.J., Alley, R.B., Zielinski, G.A., Grootes, P.M., Ram, M., Taylor, K.C., Mayewski, P.A., Bolzan, J.F., 1997. The Greenland ice sheet project 2 depth-age scale: methods and results. J. Geophys. Res. 102, 26411–26423.
Mitchell, L.E., Brook, E.J., Sowers, T., McConnell, J.R., Taylor, K., 2011. Multidecadal variability of atmospheric methane, 1000–1800 C.E. J. Geophys. Res. Biogeosci. 116, G02007.
Moore, J.C., Wolff, E.W., Clausen, H.B., Hammer, C.U., Legrand, M.R., Fuhrer, K., 1994. Electrical response of the Summit-Greenland ice core to ammonium, sulphuric acid, and hydrochloric acid. Geophys. Res. Lett. 21, 565–568.
Mortensen, A.K., Bigler, M., Grönvold, K., Steffensen, J.P., Johnsen, S.J., 2005. Volcanic ash layers from the Last Glacial Termination in the NGRIP ice core. J. Quat. Sci. 20, 209–219.
NEEM Community Members, 2013. Eemian interglacial reconstructed from a Greenland folded ice core. Nature 493, 489–494.
North Greenland Ice Core Project Members, 2004. High-resolution record of Northern Hemisphere climate extending into the Last Interglacial period. Nature 431, 147–151.
Obrochta, S.P., Yokoyama, Y., Morén, J., Crowley, T.J., 2014. Conversion of GISP2-based sediment core age models to the GICC05 extended chronology. Quat. Geochronol. 20, 1–7.
Okazaki, Y., Timmermann, A., Menviel, L., Harada, N., Abe-Ouchi, A., Chikamoto, M.O., Mouchet, A., Asahi, H., 2010. Deepwater formation in the North Pacific during the Last Glacial Termination. Science 329, 200–204.
Orsi, A.J., Cornuelle, B.D., Severinghaus, J.P., 2014. Magnitude and temporal evolution of Dansgaard-Oeschger event 8 abrupt temperature change inferred from nitrogen and argon isotopes in GISP2 ice using a new least-squares inversion. Earth Planet. Sci. Lett. 395, 81–90. http://dx.doi.org/10.1016/j.epsl.2014.03.030.
Palmer, A.S., van Ommen, T.D., Curran, M.A.J., Morgan, V.I., Souney, J.M., Mayewski, P.A., 2001. High precision dating of volcanic events (A.D. 1301–1995) using ice cores from Law Dome, Antarctica. J. Geophys. Res. 106, 28089–28095.
Panton, C., 2014. Automated mapping of local layer slope and tracing of internal layers in radio echograms. Ann. Glaciol. 55, 71–77.
Peterson, L.C., Haug, G.H., Hughen, K.A., Röhl, U., 2000. Rapid changes in the hydrologic cycle of the tropical Atlantic during the Last Glacial. Science 290, 1947–1951.
Plummer, C.T., Curran, M.A.J., van Ommen, T.D., Rasmussen, S.O., Moy, A.D., Vance, T.R., Clausen, H.B., Vinther, B.M., Mayewski, P.A., 2012. An independently dated 2000-yr volcanic record from Law Dome, East Antarctica, including a new perspective on the dating of the 1450s CE eruption of Kuwae, Vanuatu. Clim. Past 8, 1929–1940.
Ram, M., Donarummo, J., Sheridan, M., 1996. Volcanic ash from Icelandic ~57,300 Yr BP eruption found in GISP2 (Greenland) ice core. Geophys. Res. Lett. 23, 3167–3169.
Rashid, H., Hesse, R., Piper, D.J.W., 2003. Evidence for an additional Heinrich event between H5 and H6 in the Labrador Sea. Paleoceanography 18, 1077.
Rasmussen, S.O., Abbott, P.M., Blunier, T., Bourne, A.J., Brook, E., Buchardt, S.L., Buizert, C., Chappellaz, J., Clausen, H.B., Cook, E., Dahl-Jensen, D., Davies, S.M., Guillevic, M., Kipfstuhl, S., Laepple, T., Seierstad, I.K., Severinghaus, J.P., Steffensen, J.P., Stowasser, C., Svensson, A., Vallelonga, P., Vinther, B.M., Wilhelms, F., Winstrup, M., 2013. A first chronology for the North Greenland Eemian Ice Drilling (NEEM) ice core. Clim. Past 9, 2713–2730.
Rasmussen, S.O., Andersen, K.K., Svensson, A.M., Steffensen, J.P., Vinther, B.M., Clausen, H.B., Siggaard-Andersen, M.-L., Johnsen, S.J., Larsen, L.B., Dahl-Jensen, D., Bigler, M., Röthlisberger, R., Fischer, H., Goto-Azuma, K., Hansson, M.E., Ruth, U., 2006. A new Greenland ice core chronology for the Last Glacial termination. J. Geophys. Res. 111, D06102. http://dx.doi.org/10.01029/02005JD006079.
Rasmussen, S.O., Bigler, M., Blockley, S., Blunier, T., Buchardt, B., Clausen, H., Cvijanovic, I., Dahl-Jensen, D., Johnsen, S., Fischer, H., Gkinis, V., Guillevic, M., Hoek, W., Lowe, J., Pedro, J., Popp, T., Seierstad, I., Steffensen, J., Svensson, A., Vallelonga, P., Vinther, B., Walker, M., Wheatley, J.J., Winstrup, M., 2014. A stratigraphic framework for abrupt climatic changes during the Last Glacial period based on three synchronized Greenland ice-core records: refining and extending the INTIMATE event stratigraphy. Quat. Sci. Rev. 106, 14–28.
Rasmussen, S.O., Seierstad, I.K., Andersen, K.K., Bigler, M., Dahl-Jensen, D., Johnsen, S.J., 2008. Synchronization of the NGRIP, GRIP, and GISP2 ice cores across MIS 2 and palaeoclimatic implications. Quat. Sci. Rev. 27, 18–28.
Rasmussen, T.L., Wastegård, S., Kuijpers, A., Weering, T.C.E.v., Heinemeier, J., Thomsen, E., 2003. Stratigraphy and distribution of tephra layers in marine sediment cores from the Faeroe Islands, North Atlantic. Mar. Geol. 199, 263–277.
Rhodes, R., Brook, E., Chiang, J., Blunier, T., Cheng, H., Edwards, R.L., Maselli, O., McConnell, J., Romanini, D., Severinghau, J., Sowers, T., Stowasser, C., 2014. Continuous methane record of abrupt climate change 10–68 ka: sighting Heinrich events in the ice core record. Geophys. Res. Abstr. 16. EGU2014-7984.
Rosen, J.L., Brook, E.J., Severinghaus, J.P., Blunier, T., Mitchell, L.E., Lee, J.E., Edwards, J.S., Gkinis, V., 2014. An ice core record of near-synchronous global climate changes at the Bølling transition. Nat. Geosci. 7, 459–463.
Ruddiman, W.F., 1977. Late Quaternary deposition of ice-rafted sand in the subpolar North Atlantic (lat 40° to 65°N). Geol. Soc. Am. Bull. 88, 1813–1827.
Sanchez Goñi, M.F., Harrison, S.P., 2010. Millennial-scale climate variability and vegetation changes during the Last Glacial: concepts and terminology. Quat. Sci. Rev. 29, 2823–2827.
Schwander, J., Barnola, J.-M., Andrié, C., Leuenberger, M., Ludin, A., Raynaud, D., Stauffer, B., 1993. The age of the air in the firn and the ice at Summit, Greenland. J. Geophys. Res. 98, 2831–2838.
Schwander, J., Sowers, T., Barnola, J.M., Blunier, T., Fuchs, A., Malaizé, B., 1997. Age scale of the air in the summit ice: implication for glacial–interglacial temperature change. J. Geophys. Res. Atmos. 102, 19483–19493.
Schwander, J., Stauffer, B., 1984. Age difference between polar ice and the air trapped in its bubbles. Nature 311, 45–47.

Severinghaus, J.P., Beaudette, R., Headly, M.A., Taylor, K., Brook, E.J., 2009. Oxygen-18 of O_2 records the impact of abrupt climate change on the terrestrial biosphere. Science 324, 1431–1434.

Severinghaus, J.P., Brook, E.J., 1999. Abrupt climate change at the end of the Last Glacial period inferred from trapped air in polar ice. Science 286, 930–934.

Severinghaus, J.P., Sowers, T., Brook, E.J., Alley, R.B., Bender, M.L., 1998. Timing of abrupt climate change at the end of the Younger Dryas interval from thermally fractionated gases in polar ice. Nature 391, 141–146.

Southon, J., 2004. A radiocarbon perspective on Greenland ice-core chronologies: can we use ice cores for ^{14}C calibration? Radiocarbon 46, 1239–1259.

Stanford, J.D., Rohling, E.J., Bacon, S., Roberts, A.P., Grousset, F.E., Bolshaw, M., 2011. A new concept for the paleoceanographic evolution of Heinrich event 1 in the North Atlantic. Quat. Sci. Rev. 30, 1047–1066.

Steffensen, J.P., Andersen, K.K., Bigler, M., Clausen, H.B., Dahl-Jensen, D., Fischer, H., Goto-Azuma, K., Hansson, M., Johnsen, S.J., Jouzel, J., Masson-Delmotte, V., Popp, T., Rasmussen, S.O., Röthlisberger, R., Ruth, U., Stauffer, B., Siggaard-Andersen, M.-L., Sveinbjörnsdóttir, Á.E., Svensson, A., White, J.W.C., 2008. High-resolution Greenland ice core data show abrupt climate change happens in few years. Science 321, 680–684.

Steig, E.J., Grootes, P.M., Stuiver, M., 1994. Seasonal precipitation timing and ice core records. Science 266, 1885–1886.

Stuiver, M., Grootes, P.M., 2000. GISP2 oxygen isotope ratios. Quat. Res. 53, 277–284.

Svensson, A., Andersen, K.K., Bigler, M., Clausen, H.B., Dahl-Jensen, D., Davies, S.M., Johnsen, S.J., Muscheler, R., Parrenin, F., Rasmussen, S.O., Röthlisberger, R., Seierstad, I., Steffensen, J.P., Vinther, B.M., 2008. A 60 000 year Greenland stratigraphic ice core chronology. Clim. Past 4, 47–57.

Svensson, A., Andersen, K.K., Bigler, M., Clausen, H.B., Dahl-Jensen, D., Davies, S.M., Johnsen, S.J., Muscheler, R., Rasmussen, S.O., Röthlisberger, R., Steffensen, J.P., Vinther, B.M., 2006. The Greenland ice core chronology 2005, 15–42 ka. Part 2: comparison to other records. Quat. Sci. Rev. 25, 3258–3267.

Svensson, A., Bigler, M., Blunier, T., Clausen, H.B., Dahl-Jensen, D., Fischer, H., Fujita, S., Goto-Azuma, K., Johnsen, S.J., Kawamura, K., Kipfstuhl, S., Kohno, M., Parrenin, F., Popp, T., Rasmussen, S.O., Schwander, J., Seierstad, I., Severi, M., Steffensen, J.P., Udisti, R., Uemura, R., Vallelonga, P., Vinther, B.M., Wegner, A., Wilhelms, F., Winstrup, M., 2013. Direct linking of Greenland and Antarctic ice cores at the Toba eruption (74 ka BP). Clim. Past 9, 749–766.

Taylor, K.C., Alley, R.B., Lamorey, G.W., Mayewski, P., 1997. Electrical measurements on the Greenland ice sheet project 2 core. J. Geophys. Res. 102, 26511–26517.

Taylor, K.C., Hammer, C.U., Alley, R.B., Clausen, H.B., Dahl-Jensen, D., Gow, A.J., Gundestrup, N.S., Kipfstuhl, J., Moore, J.C., Waddington, E.D., 1993a. Electrical conductivity measurements from the GISP2 and GRIP Greenland ice cores. Nature 366, 549–552.

Taylor, K.C., Lamorey, G.W., Doyle, G.A., Alley, R.B., Grootes, P.M., Mayewski, P.A., White, J.W.C., Barlow, L.K., 1993b. The "flickering switch" of late Pleistocene climate change. Nature 361, 432–436.

Taylor, K.C., Mayewski, P.A., Twickler, M.S., Whitlow, S.I., 1996. Biomass burning recorded in the GISP2 ice core: a record from eastern Canada? Holocene 6, 1–6.

Vinther, B.M., Buchardt, S.L., Clausen, H.B., Dahl-Jensen, D., Johnsen, S.J., Fisher, D.A., Koerner, R.M., Raynaud, D., Lipenkov, V., Andersen, K.K., Blunier, T., Rasmussen, S.O., Steffensen, J.P., Svensson, A.M., 2009. Holocene thinning of the Greenland ice sheet. Nature 461, 385–388.

Vinther, B.M., Clausen, H.B., Johnsen, S.J., Rasmussen, S.O., Andersen, K.K., Buchardt, S.L., Dahl-Jensen, D., Seierstad, I.K., Siggaard-Andersen, M.-L., Steffensen, J.P., Svensson, A.M., Olsen, J., Heinemeier, J., 2006. A synchronized dating of three Greenland ice cores throughout the Holocene. J. Geophys. Res. 111, D13102. http://dx.doi.org/10.11029/12005JD006921.

Wang, Y.J., Cheng, H., Edwards, R.L., An, Z.S., Wu, J.Y., Shen, C.C., Dorale, J.A., 2001. A high-resolution absolute-dated Late Pleistocene monsoon record from Hulu Cave, China. Science 294, 2345–2348.

Werner, M., Heimann, M., Hoffmann, G., 2001. Isotopic composition and origin of polar precipitation in present and glacial climate simulations. Tellus Ser. B Chem. Phys. Meteorol. 53, 53–71.

Werner, M., Mikolajewicz, U., Heimann, M., Hoffmann, G., 2000. Borehole versus isotope temperatures on Greenland: seasonality does matter. Geophys. Res. Lett. 27, 723–726.

Wolff, E.W., Chappellaz, J., Blunier, T., Rasmussen, S.O., Svensson, A., 2010. Millennial-scale variability during the Last Glacial: the ice core record. Quat. Sci. Rev. 29, 2828–2838.

Wolff, E.W., Moore, J.C., Clausen, H.B., Hammer, C.U., 1997. Climatic implications of background acidity and other chemistry derived from electrical studies of the Greenland Ice Core Project ice core. J. Geophys. Res. 102, 26325–26332.

Zielinski, G.A., Mayewski, P.A., Meeker, D., Grönvold, K., Germani, M.S., Whitlow, S., Twickler, M.S., Taylor, K., 1997. Volcanic aerosol records and tephrachronology of the Summit, Greenland, ice cores. J. Geophys. Res. 102, 26625–26640.